European Journal of Medicinal Chemistry 302 (2026) 118369

Contents lists available at ScienceDirect

European Journal of Medicinal Chemistry

journal homepage: www.elsevier.com/locate/ejmech

Research paper

Fine-tuning 5-HT$_7$ receptor selectivity, inverse agonism, and metabolic stability of new (aryloxy)ethyl-piperidines toward antidepressant and pro-cognitive properties

Vittorio Canale [a,*], Klaudia Blicharz-Futera [a,d], Monika Bijata [e], Natalie G. Cavalco [f], Anna Partyka [b], Matylda Stefaniak [a], Michał Kamiński [a,d], Grzegorz Satała [h], Dawid Warszycki [h], Janelle K. Lanham [f], Joanna Gołębiowska [i], Maciej Gawlik [c], Magdalena Smolik [c], Krystian Bijata [e], Magdalena Jastrzębska-Więsek [b], Rafał Kurczab [h], Andrzej J. Bojarski [h], Maria Walczak [c], John D. McCorvy [f,g], Jakub Włodarczyk [e], Piotr Popik [i], Paweł Zajdel [a]

[a] Department of Organic Chemistry, Jagiellonian University Medical College, 9 Medyczna Str., 30-688, Krakow, Poland
[b] Department of Clinical Pharmacy, Jagiellonian University Medical College, 9 Medyczna Str., 30-688, Krakow, Poland
[c] Department of Toxicology, Jagiellonian University Medical College, 9 Medyczna Str., 30-688, Krakow, Poland
[d] Doctoral School of Medical and Health Sciences, Jagiellonian University Medical College, 16 St. Łazarza Str., 31-530, Krakow, Poland
[e] Laboratory of Cell Biophysics, Nencki Institute of Experimental Biology, 3 Pasteur Str., 02-093, Warsaw, Poland
[f] Department of Cell Biology, Neurobiology & Anatomy, Neuroscience Research Center, Cancer Center, Medical College of Wisconsin, 8701 Watertown Plank Rd., Milwaukee, WI, 53226, United States
[g] Department of Pharmacology and Toxicology, Neuroscience Research Center, Cancer Center, Medical College of Wisconsin, 8701 Watertown Plank Rd., Milwaukee, WI, 53226, United States
[h] Department of Medicinal Chemistry, Institute of Pharmacology, Polish Academy of Sciences, 12 Smętna Str., 31-343, Krakow, Poland
[i] Department of Behavioral Neuroscience & Drug Development, Institute of Pharmacology, Polish Academy of Sciences, 12 Smętna Str., 31-343, Krakow, Poland

ARTICLE INFO

Keywords:
5-HT$_7$ receptor inverse agonists
MMP-9
Antidepressant-like effects
Pro-cognitive properties
Affective disorders

ABSTRACT

Affective disorders, the leading causes of disability and premature death worldwide, require new and effective treatment strategies. Clinically used antidepressants and second-generation antipsychotic drugs, including vortioxetine and lurasidone, act as potent 5-HT$_7$ receptor antagonists and improve cognitive functions in the patients with mood disorders. Additionally, 5-HT$_7$ receptor-mediated activation of matrix metalloproteinase 9 (MMP-9) induces depressive-like behavior in mice. We designed and synthesized a series of 27 arylsulfonamide derivatives of 2-[(2-aryl/2-heteroaryl)phenoxy]ethyl-piperidines and examined their *in vitro* and *in vivo* effects. These compounds are closely related to the previously reported 5-HT$_7$ receptor ligand (PZ-1129), developed in our laboratories. Our goal was to investigate the impact of heterocyclic ring replacement on receptor selectivity and metabolic stability, because the aryloxyl moiety was postulated to determine affinity for serotonin and dopamine receptors, and interactions with metabolizing enzymes. The study identified compound **57** as a potent, selective and metabolically stable 5-HT$_7$ receptor inverse agonist of Gs signaling pathway. Bioavailable compound **57** shortened immobility in the forced swim test in mice and reversed PCP-induced cognitive deficits in the novel object recognition test in rats suggesting antidepressant-like and pro-cognitive effects. In addition, compound **57** reduced 5-HT$_7$ receptor-mediated MMP-9 activity in the mouse hippocampus with efficacy comparable to the reference 5-HT$_7$ receptor antagonist, SB-269970, further suggesting its purported antidepressant-like actions. These findings support the potential therapeutic application of targeting 5-HT$_7$ receptor/MMP-9 signaling pathway for the treatment of affective disorders.

* Corresponding author. Department of Organic Chemisty, Jagiellonian University Medical College, 9 Medyczna Str., 30-688, Kraków, Poland.
E-mail address: vittorio.canale@uj.edu.pl (V. Canale).

https://doi.org/10.1016/j.ejmech.2025.118369
Received 15 May 2025; Received in revised form 6 November 2025; Accepted 10 November 2025
Available online 21 November 2025
0223-5234/© 2025 Published by Elsevier Masson SAS.

1. Introduction

Many antidepressant and second-generation antipsychotic drugs, which are used for the treatment of depression, demonstrate high affinity for the serotonin type 7 (5-HT$_7$) receptor. Among these, vortioxetine and lurasidone, which act as 5-HT$_7$ receptor antagonists, have been shown to improve cognitive functioning in patients with major depressive disorder (MDD) [1,2]. In addition, preclinical studies in rodents suggest that 5-HT$_7$ receptor antagonists may be a promising option for treating anxiety disorders and neurodegenerative diseases [3,4].

The 5-HT$_7$ receptor belongs to the G protein-coupled receptor (GPCR) family and is positively coupled to Gs protein, which activates adenylyl cyclase, increasing intracellular level of cyclic AMP [5]. Additionally, it is coupled to the G_{12} protein, which activates small GTPases of the Rho family [6]. Moreover, 5-HT$_7$ receptor exhibits a high level of constitutive activity at Gs signaling pathway. The 5-HT$_7$ receptor is predominantly located in the functionally relevant brain areas, i.e., thalamus, hypothalamus, hippocampus, prefrontal cortex and dorsal raphe nucleus. Notably, the 5-HT$_7$ receptor demonstrates high homology (ca. 90 %) across species, while exhibiting similarity only with serotonin 5-HT$_{1A}$ receptor subtype. Blockade of 5-HT$_7$ receptor's constitutive activity either through genetic knockout or administration of 5-HT$_7$ receptor inverse agonist resulted in a decrease in matrix metalloproteinase 9 (MMP-9) activity in the mouse hippocampus [7]. Elevated levels of MMP-9 have been also detected in the blood of patients diagnosed with major depression, further establishing this enzyme as one of the most reliable biomarkers for depression [8].

Previous efforts have been largely unsuccessful in identifying potent and selective antagonists of the 5-HT$_7$ receptor that demonstrate clinical efficacy. To date, JNJ-18038683 the only selective 5-HT$_7$ receptor antagonist has progressed to phase II clinical trials for depression treatment [9]. Another study assessed the potential pro-cognitive effects of JNJ-18038683 in patients with bipolar disorder, but the findings were inconclusive [10].

Our contribution to the quest for 5-HT$_7$ receptor antagonists involved the development of a distinguished class of arylsulfonamides derived from (aryloxy)alkyl-alicyclic amines, designed as flexible biomimetics that effectively replace long-chain arylpiperazines (LCAP) [11]. This strategy involved substitution of the arylpiperazine moiety with (aryloxy)ethyl-amin fragments, while simultaneously introducing partial rigidification within the alkylene chain. These modifications apply the bioisosteric principle by replacing amide/imide linkages found in LCAP's with sulfonamide group. The resulting compounds e.g., PZ-766, PZ-1404 [12] and PZ-1433 [13] have demonstrated significant antidepressant-like and pro-cognitive properties in preclinical models, underscoring their purported therapeutic effects [14,15]. However, we cannot exclude the possibility that other targets e.g., serotonin 5-HT$_{1A}$ and dopamine D_2 receptors, contribute to the observed *in vivo* effects. In addition, *in vitro* biotransformation studies revealed that derivatives containing either unsubstituted phenyl ring or an isopropyl group in *ortho* position at the aryloxy fragment were more susceptible to enzymatic hydroxylation.

This relative unselective profile, combined with high metabolic liability prompted us to develop novel, selective, and metabolically stable 5-HT$_7$ receptor inverse agonists that could better elucidate the therapeutic role of 5-HT$_7$ receptor in treating affective disorders.

To address these challenges, we designed, supported by *in silico* methods, and synthesized a focused 27-member library of 4-fluorobenzensulfonamide derivatives of 2-[(2-aryl/2-heteroaryl)phenoxy]ethyl-piperidines as close analogs of previously reported compound PZ-1129 (Fig. 1) [12]. Specifically, we introduced small substituents at the distal phenyl ring of PZ-1129 to sterically hinder potential metabolic hotspots and modulate electronic density. Additionally, we incorporated selected five- and six-membered heterocyclic moieties to decrease the overall lipophilicity and mitigate oxidative metabolism.

Moreover, we examined the effect of synthesized compounds on 5-HT$_7$ receptor-dependent Gs signaling pathway. We assessed the antidepressant-like properties of the most potent compound using the forced swim test (FST) and tail suspension test (TST) in mice. Finally, we investigated the impact of selected compound **57** on 5-HT$_7$ receptor-mediated MMP-9 activity in mice hippocampi using *ex vivo* assays and determined its cognitive properties in the novel object recognition (NOR) test in rats.

2. Results and discussion

2.1. In silico experiments

The design of compounds was guided by *in silico* methods using a hierarchical multistep protocol. This included assessment of physicochemical (logP, TPSA, pK_a, CNS-MPO) and ADME properties (*i.e.* brain-blood barrier penetration, metabolic stability), a machine learning process and molecular docking to homology models of the 5-HT$_7$ receptor and selectivity prediction model for structurally related 5-HT$_{1A}$ receptor. Applying the sum rank method for data fusion across all scores determined by employed filters, we were able to rank designed compounds by the best predicted activity and suitable ADME properties identifying the most promising building blocks for the synthesis. Specifically, only compounds that exhibited a high-scoring docked binding mode for 5-HT$_7$ receptor (Glide Gscore < -6) in hybrid homology models for GPCR, together with adequate predicted values for blood-brain barrier penetration (BBB score ≥ 3) and metabolic stability (#metab score <5), were selected for synthesis (Table 1–SI). Conversely, compounds demonstrating high scoring docked binding modes at the 5-HT$_{1A}$ and D_2 receptors (Glide Gscore > -8) or failing to meet ADME criteria (BBB score <3 and #metab ≥ 5) were excluded from further consideration (Table 1–SI). Moreover, to confirm differences in the binding modes of selected compound and PZ-1129 in D_2 receptor binding pocket, molecular dynamics simulations were performed.

2.2. Synthesis

The newly designed 4-fluorobenzenesulfonamide derivatives of 2-[(2-aryl/2-heteroaryl)phenoxy]ethyl-piperidines **31**–**57** were

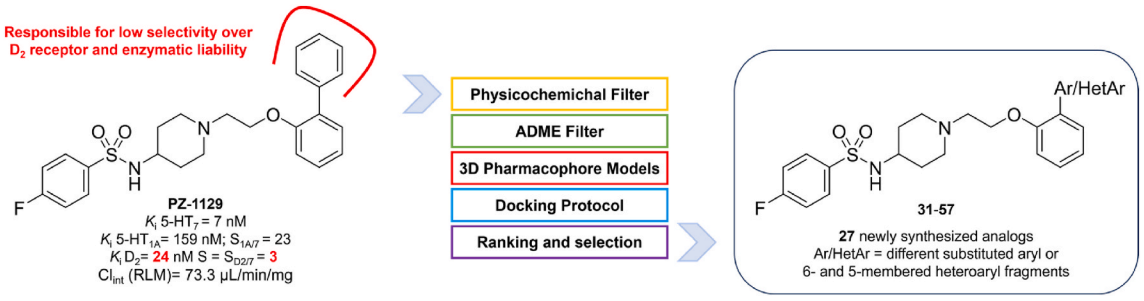

Fig. 1. Design strategy for a limited library of 4-fluorobenzenesulfonamide derivatives of 2-[(2-aryl/2-heteroaryl)phenoxy]ethyl-piperidines.

synthesized according to a multistep procedure (Scheme 1) integrating classic organic synthesis with mechanochemistry [12,16]. Briefly, the commercially available 2-iodophenol **1** was treated with 1,2-dibromoethane in the presence of potassium carbonate to afford (aryloxy)ethyl bromide **2**. Through a subsequent alkylation of 4-(*N*-Boc-amino)piperidine with **2** in a vibratory ball mill (vbm) for 1 h, intermediate **3** was obtained in 88 % yield. This intermediate underwent a Suzuki cross-coupling reaction with differently substituted aryl/heteroaryl boronic acids or esters and $Pd(PPh_3)_4$ as catalyst producing **4**–**30** in yields ranging from 58 to 98 %.

Final arylsulfonamide derivatives **31**–**57** were obtained using a sustainable one-pot two-step deprotection/sulfonylation mechanochemical procedure [17]. According to this protocol, Boc-protected intermediates **4**–**30** were milled with 6 M HCl solution in isopropanol (*i*Pr-OH) for 30 min using 35 mL PTFE jars, following by the addition of potassium carbonate as grinding auxiliary and a slightly excess of 4-fluorobenzenesulfonyl chloride (yields: 75–93 %).

2.3. *In vitro assessment of 5-HT$_7$ receptor affinity and selectivity profile*

All newly synthesized compounds **31**–**57** were tested in the competition binding experiments for human 5-HT_7, 5-HT_{1A}, and D_2 receptors, stably expressed in HEK293 cells, according to the previously published procedures [18]. Using the unsubstituted derivative PZ-1129, as our molecular template, we initially explored effects of various electron-donating and withdrawing substituents at the distal phenyl ring of the aryloxy fragment. We found that substituents such as fluorine, methoxy and methyl groups – regardless of their position (2-, 3- or 4-position) – decreased the affinity for 5-HT_7 receptor compared to PZ-1129 (Table 1). In terms of selectivity over 5-HT_{1A} and D_2 receptors, only 2-fluoro and 3-methoxy maintained a comparable selectivity ratio to unsubstituted compound. Next, substituting the five aromatic hydrogen atoms in the PZ-1129 compound with their heavier deuterium isotopes, led to a potent 5-HT_7 receptor ligand **39**, which exhibited improved selectivity over 5-HT_{1A} receptor. However, its high affinity for the D_2 receptor did not align with our criteria for further consideration.

Recognizing bioisosteric replacement as an effective strategy to enhance pharmacological efficacy and optimize pharmacokinetic properties through improving metabolic stability [19], we examined the effects of differently substituted six- or five-membered heteroaryl moieties on their interaction with evaluated biological targets. We observed that replacing phenyl ring with 3- or 4-pyridyl fragments conferred high affinity for 5-HT_7 receptor, while substitution with 2-pyridyl group did not yield similar benefits. Of note, compounds **41** and **42** displayed, as compared with PZ-1129, a lower affinity (K_i = 13 and 17 nM), for 5-HT_7 receptor, respectively, along with high selectivity over 5-HT_{1A} receptor subtype, achieving ratios of up to 50-fold.

These findings align with *in silico* simulations, which suggest that both compounds exhibit a binding mode similar to that of the parent compound PZ-1129 (Fig. 2A), preserving key interactions in the 5-HT_7 receptor binding pocket that contribute to their high potency. Notable interactions include a salt bridge with aspartate D3.32, π-π stacking with tryptophan W6.48, and specific interactions with phenylalanine F5.47 (for compound **41**) or F6.52 (for compound **42**). Furthermore, the presence of a nitrogen atom at 4-position – rather than at the 3-position – drastically reduced the selectivity over D_2 receptor, resulting in compound **42** acting as a dual 5-HT_7/D_2 receptor ligand. The high affinity of compound **42** for D_2 receptors (K_i = 16 nM) can be attributed to the heteroaryl fragment being positioned deeper in the binding pocket. This alters the orientation of the arylsulfonamide terminal fragment and enables the formation of a hydrogen bond with the isoleucine residue in the extracellular loop 2 ($I184^{ECL2}$). This additional stabilization of the receptor-ligand complex was not observed for the 3-pyridyl analog (compound **41**, Fig. 2B).

Given the favorable effects of 3-pyridyl moiety, we then sought to enhance the selectivity of pyridine-containing compound **41** by introducing a methoxy group and fluorine atom at available position at the heteroaromatic ring. In contrast to other tested derivatives, only compounds **44** (4-methoxy-3-pyridyl) and **45** (5-methoxy-3-pyridyl) exhibited equipotent affinity to the parent compound at 5-HT_7 receptor whereas the former demonstrated high selectivity over 5-HT_{1A} receptor (a selectivity ratio of 96-fold). Molecular docking studies indicated that the biaryl fragment of compound **44** could not fit into the hydrophobic cluster formed by TM5 and TM6 helices in the 5-HT_{1A} receptor pocket, resulting in a reversal of the binding mode (Fig. 1–SI). Introduction of fluorine atom at 2- or 5-position of the pyridine moiety led to potent 5-HT_7 receptor ligands **47** and **48** (K_i = 11 and 29 nM, respectively) yet displaying poorer selectivity over D_2 receptor.

We further discovered that the position of the heteroatom (N, O or S) within five-membered aryl moieties plays a critical role in the interaction with the biological targets. In contrast to compounds bearing 2-pyrrolyl (**49**), 2-*N*-methyl-pyrrolyl (**50**), 2-furanyl (**51**) and 2-pyrazolyl (**53**), only the 2-thienyl moiety resulted in the highly potent 5-HT_7 receptor ligand **52**, which exhibits selectivity over 5-HT_{1A} and D_2 receptors (selectivity ratios of 43 and 16, respectively). We then found that shifting heteroatom from 2- to 3-position within the aryl moiety, regardless of the specific heteroatom, was beneficial for enhancing interaction with the 5-HT_7 receptor (**53** *vs.* **56** and **57**, **51** *vs.* **54** and **52** *vs.* **55**) providing the potent ligands with K_i values below 20 nM (Fig. 2C).

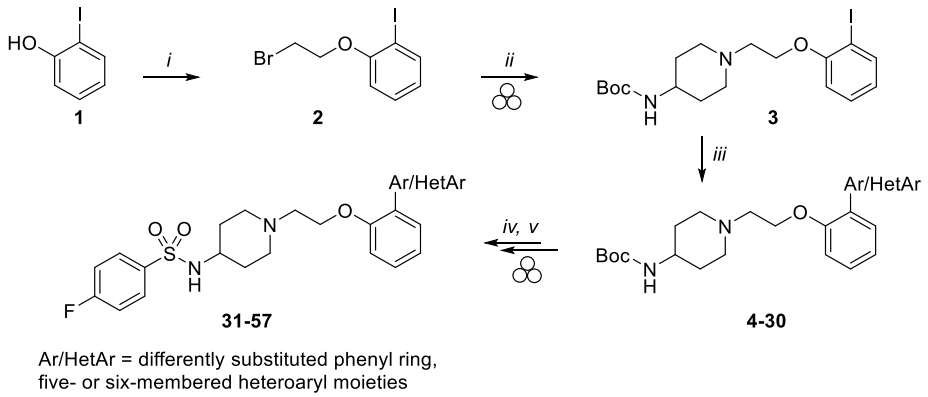

Scheme 1. Synthesis of the 4-fluorobenzenesulfonamide derivatives of 2-[(2-aryl/2-heteroaryl)phenoxy]ethyl-piperidines **31**–**57**. Reagents and conditions: *i*) 1,2-dibromoethane (4 eq), K_2CO_3 (3 eq), KI (cat.), Acetone, 60 °C, 48 h (yield: 69 %), *ii*) vibratory ball mill (vbm) 35 mL PTFE jar, φ_{ball} = 1.5 cm, 4-(Boc-*N*-amino)-piperidine (1 eq), K_2CO_3 (3 eq), rt, 1 h (yield: 88 %); *iii*) differently substituted aryl/heteroaryl boronic acids or esters (1.2 eq), $Pd(PPh_3)_4$ (0.5 eq), K_2CO_{3sat}, dioxane, MW, 140 °C, 2 h (yields: 58–98 %), *iv*) vbm, 30 Hz, 35 mL PTFE jar, φ_{ball} = 1.5 cm, 6 M HCl in *i*Pr-OH (10 eq) 30 min, then *v*) K_2CO_3 (25 eq), 4-fluorobenzenesulfonyl chloride (1.1 eq), rt, 5 min (yields: 75–93 %).

Table 1
The binding data of synthesized compounds **31**–**57**, in-house reference compounds PZ-1129, PZ-1404 and reference ligand SB-269970 at 5-HT_7, 5-HT_{1A} and D_2 receptors.

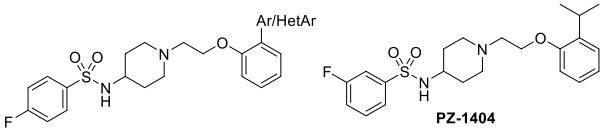

Compound	Ar/ HetAr	K_i [nM] (pK_i ± SEM)[a]			S_{1A} \7[b]	S_{D2} \7[c]
		5-HT_7 receptor	5-HT_{1A} receptor	D_2 receptor		
PZ-1129		7 (8.16 ± 0.06)	159 (6.80 ± 0.07)	24 (7.63 ± 0.07)	23	3
31		35 (7.46 ± 0.09)	572 (6.25 ± 0.07)	45 (7.36 ± 0.09)	16	1
32		204 (6.70 ± 0.07)	1566 (5.81 ± 0.07)	37 (7.44 ± 0.07)	8	<1
33		51 (7.30 ± 0.07)	627 (6.21 ± 0.07)	58 (7.24 ± 0.07)	12	2
34		52 (7.29 ± 0.07)	703 (6.16 ± 0.07)	73 (7.15 ± 0.09)	14	1
35		30 (7.53 ± 0.09)	960 (6.02 ± 0.07)	70 (7.16 ± 0.07)	32	2
36		61 (7.22 ± 0.07)	412 (6.39 ± 0.07)	143 (6.85 ± 0.06)	7	2
37		106 (6.98 ± 0.07)	1043 (5.99 ± 0.07)	103 (6.99 ± 0.08)	10	1
38		80 (7.10 ± 0.07)	861 (6.07 ± 0.07)	93 (7.04 ± 0.07)	11	1
39		16 (7.81 ± 0.11)	848 (6.08 ± 0.06)	61 (7.22 ± 0.09)	53	4
40		115 (6.94 ± 0.07)	4392 (5.36 ± 0.07)	587 (6.24 ± 0.07)	38	5
41		13 (7.89 ± 0.07)	651 (6.19 ± 0.07)	114 (6.95 ± 0.07)	50	9
42		17 (7.78 ± 0.08)	765 (6.12 ± 0.07)	16 (7.80 ± 0.05)	45	<1
43		109 (6.97 ± 0.06)	822 (6.09 ± 0.07)	120 (6.93 ± 0.07)	8	1
44		15 (7.83 ± 0.06)	1446 (5.84 ± 0.07)	108 (6.97 ± 0.06)	96	7
45		19 (7.73 ± 0.07)	416 (6.39 ± 0.07)	193 (6.72 ± 0.07)	22	10
46		69 (7.17 ± 0.06)	493 (6.31 ± 0.07)	348 (6.46 ± 0.07)	7	5
47		11 (7.97 ± 0.08)	406 (6.40 ± 0.07)	70 (7.16 ± 0.07)	37	7
48		29 (7.54 ± 0.06)	798 (6.10 ± 0.07)	289 (6.54 ± 0.07)	28	10
49		1249 (5.91 ± 0.07)	26710 (4.58 ± 0.07)	1302 (5.89 ± 0.07)	21	1
50		148 (6.83 ± 0.07)	971 (6.02 ± 0.07)	239 (6.63 ± 0.07)	7	1
51		159 (6.80 ± 0.07)	2535 (5.60 ± 0.07)	2379 (5.63 ± 0.07)	16	15
52		29 (7.54 ± 0.06)	1237 (5.91 ± 0.07)	476 (6.33 ± 0.07)	43	16
53		166 (6.78 ± 0.07)	6833 (5.17 ± 0.07)	177 (6.76 ± 0.07)	41	1
54		20 (7.70 ± 0.07)	1571 (5.81 ± 0.07)	418 (6.38 ± 0.07)	79	21
55		18 (7.75 ± 0.07)	619 (6.21 ± 0.07)	154 (6.82 ± 0.07)	34	9
56		5 (8.31 ± 0.07)	99 (7.01 ± 0.07)	899 (6.05 ± 0.07)	20	180
57		5 (8.31 ± 0.06)	292 (6.54 ± 0.07)	1004 (6.00 ± 0.06)	58	200
PZ-1404[d]		10 (8.00 ± 0.05)	378 (6.42 ± 0.06)	112 (6.95 ± 0.05)	38	11
SB-269970		3 (8.52 ± 0.02)	>1000 (<6)	714 (6.15 ± 0.07)	>300	238

[a] Mean K_i and pK_i values ± SEMs (standard error of the mean) based on three independent binding experiments in HEK293 cells stably expressing h5-HT_7, h5-HT_{1A}, hD_2 receptors.
[b] Ratio of affinity for h5-HT_{1A} receptor *vs* h5-HT_7 receptor.
[c] Ratio of affinity for hD_2 receptor *vs* h5-HT_7 receptor.
[d] Compound 10 from Ref. [12].

Finally, the replacement of phenyl moiety in PZ-1129 with 3-pyrazolyl or *N*-methyl-3-pyrazolyl considerably improved selectivity over D_2 receptors (180 and 200-fold, respectively). *In silico* simulations revealed that, unlike PZ-1129, compound **57** did not accurately fit into the D_2 receptor binding pocket (as evidenced by the inversion of the binding mode of new compound, Fig. 2D), resulting in a drop in potency at D_2 receptor. In line with molecular docking studies, 200 ns-long molecular dynamic simulations [20], followed by the analysis of changes in the ligand-protein contacts (Fig. 10–SI), confirmed that the biphenyl moiety of compound PZ-1129 is deeply embedded within the hydrophobic cluster of the D_2 receptor binding pocket. This optimal special occupation of the available space is likely a key factor contributing to the compound's enhanced affinity ($K_i = 24$ nM). In contrast, the corresponding structural fragment in compound **57** adopts a distinct orientation within the binding site and fails to engage the same hydrophobic sub-pocket, resulting in a loss of affinity ($K_i = 1004$ nM). This marked divergence in binding poses provides an explanation for the observed differences in receptor selectivity.

Structure-activity relationship studies identified compounds **56** and **57** as promising candidates, both exhibiting higher affinity for 5-HT_7 receptor ($K_i = 5$ nM) and improved selectivity over 5-HT_{1A} and D_2 receptors ($S_{1A/7} > 20$ and $S_{D2/7} > 180$) compared to the parent compound PZ-1129. Of note, compound **57** showed a superior selectivity profile relative to the previously evaluated derivative PZ-1404 and compared to that for the reference ligand SB-267790.

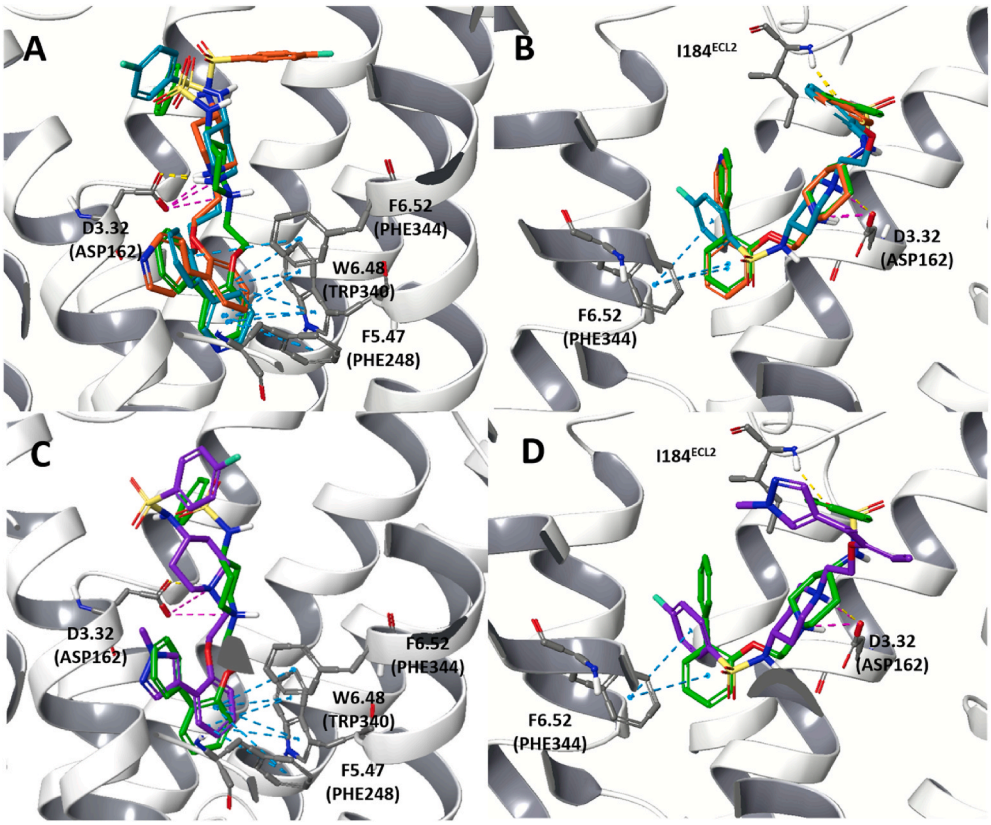

Fig. 2. A–D. A) Comparison of a binding mode of PZ-1129 (green), **41** (turquoise) and **42** (orange) in 5-HT_7 receptor binding pocket; B) Comparison of a binding mode of PZ-1129 (green), **41** (turquoise) and **42** (orange) in D_2 receptor binding pocket; C) Comparison of a binding mode of PZ-1129 (green) and **57** (violet) in 5-HT_7 receptor binding pocket; D) Comparison of a binding mode of PZ-1129 (green) and **57** (violet) in D_2 receptor binding pocket. Pink, blue and yellow dashed lines indicate salt bridges (with D3.32 residue), aromatic interactions (with F5.47, F6.52 and W6.48 in 5-HT_7 receptor; with F6.52 in D_2 receptor) and hydrogen bonds (with $I184^{ECL2}$ in D_2 receptor), respectively. Only residues which interact with ligands are visible. Receptor surface is rendered in colors corresponding to residue property. Detailed binding modes in form of ligand interaction diagrams can be found in Supporting Information (Figs. 2–8-SI). (For interpretation of the references to color in this figure legend, the reader is referred to the Web version of this article.)

2.4. *Compounds **56** and **57** show favorable in vitro metabolic stability*

In vitro assessment of ADME properties represents a key factor in selecting compounds for further *in vivo* preclinical development. Accordingly, we examined the metabolic stability of the most promising compounds **54**, **56** and **57** using QikProp software, Metasite 6 software [21] and rat liver microsomes (Table 2). Parent compound PZ-1129, PZ-1404 and reference SB-269970 were used as comparators while imipramine, a drug known for extensive metabolism (Cl_{int} = 102.7 μL/min/mg), was used as positive control. Results of *in silico* metabolic stability predictions revealed that compounds **54**, **56** and **57** displayed fewer sites of metabolisms compared to PZ-1129 (for further information, see Figs. 11–14-SI and Table 1–SI), suggesting a reduced susceptibility to enzymatic degradation. These findings were confirmed by *in vitro* evaluation. After 60 min of incubation, compound **57** exhibited a slightly higher clearance value than its close analog **56**, with Cl_{int} values of 41.6 and 30.9 μL/min/mg, respectively. In line with *in silico* simulation, compound **54**, with the 3-furanyl moiety, was strongly susceptible to enzymatic metabolism, displaying the highest clearance value (Cl_{int} = 68.4 μL/min/mg). Nevertheless, all tested derivatives showed improved stability compared to the parent compounds PZ-1129 and PZ-1404 as well as reference SB-269970 (Cl_{int} = 73.7, 124 and 99.0 μL/min/mg, respectively), indicating that the incorporation of a heteroaryl fragment into the molecular structure effectively mitigates the challenge of poor metabolic stability.

Table 2
Metabolic stability of compounds **54**, **56**, **57**, PZ-1129, PZ-1404, SB-269970 and imipramine in rat liver microsomes.

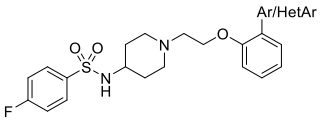

Compound	Ar/ HetAr	$t_{1/2}$ [min]	Cl_{int} (μL/min/mg)[a]	Major metabolic pathway[b]
PZ-1129		18.7	73.3	Hydroxylation
54		20.3	68.4	Hydroxylation
56		44.8	30.9	Not determined
57		33.3	41.6	*N*-demethylation
PZ-1404[c]		11.6	119.4	Hydroxylation
SB-269970		14.0	99.0	Hydroxylation
Imipramine		13.5	102.7	*N*-demethylation

[a] Determined in the RLM assay at a protein concentration of 0.5 mg/mL.
[b] Assessed by UPLC/MS analysis. Results are means of two independent experiments run in duplicate.

2.5. Compounds 56 and 57 behave as inverse agonists at 5-HT$_7$ receptor-operating Gs signaling

In the first step of assessment of compounds' functional activity, we evaluated the antagonist properties of metabolically stable compounds **56**, **57**, and parent compound PZ-1129 at 5-HT$_7$ receptor using a cell-based cAMP assay with 5-HT as agonist positive control. Similarly to the reference SB-269970 (K_B = 0.81 nM, Table 3), all compounds inhibited the agonist-induced cAMP production, classifying them as potent antagonists with K_B values lower than 3 nM (Table 3, Fig. 15–SI).

Next, we investigated the ability of compounds **56** and **57** to inhibit the constitutive activity of 5-HT$_7$ receptor using transiently transfected HEK293 cells containing 5-HT$_7$R and GloSensor to detect cAMP levels by luminescence. The compounds reduced basal cAMP production, demonstrating potent inverse agonist properties with EC$_{50}$ values 1.92 nM for compound **56** and 2.93 nM for **57** (Table 3, Fig. 3). Of note, newly developed derivatives displayed similar potency to the reference compound SB-269970 (EC$_{50}$ = 0.97 nM), while showing greater potency compared to in-house reference PZ-1129 and PZ-1404 (EC$_{50}$ = 13.7 and 27.7 nM, respectively) and drug lurasidone (EC$_{50}$ = 7.7 nM).

Given the functional activity at 5-HT$_{1A}$ and/or D$_2$ receptors may influence the pharmacological outcomes observed in *in vivo* behavioral studies, we further assessed the agonist/antagonist profile of the selected compounds and reference ligands at these sites using *in vitro* assays (Table 4). None of the tested compounds exhibited stimulatory activity at both receptors in the agonist mode. In contrast, compounds **56** and **57** slightly increased cAMP production behaving as weak 5-HT$_{1A}$ receptor antagonists in this cellular assay (K_B = 170 and 197 nM for **56** and **57**, respectively), while showing only marginal inhibitory activity at D$_2$ sites (K_B > 790 nM). Of note, the new analogs were less potent than in-house reference compounds PZ-1129 and PZ-1404 across all functional assays, suggesting that compounds **56** and **57** possess superior selectivity for the 5-HT$_7$ receptor (exceeding 67-fold selectivity over 5-HT$_{1A}$ and D$_2$ receptors).

Additional binding profile assessments confirmed high selectivity of these compounds over 5-HT$_{2A}$ and 5-HT$_6$ receptors (selectivity index >30, Table 4).

Finally, we determined the functional activity of compounds **57** and **56** at mouse and rat orthologs compared to human species of the 5-HT$_7$ receptor. The compound was equipotent across all tested species (Fig. 4), indicating a low risk of species-dependent pharmacological variability and supporting its translational relevance in animal models.

2.6. Compound 57 displayed modest inhibition of hERG channel and CYP3A4 isoform

Cardiac arrhythmias represent one of the most common adverse effects leading to drug candidate failure, often due to inhibition of the *h*ERG potassium channel. Therefore, the potential of compound **57** to interfere with *h*ERG channel activity was investigated at Eurofins Discovery (detailed results and methodology are reported at Table 2–SI), using terfenadine as a reference inhibitor (IC$_{50}$ = 52 nM). Results demonstrated that evaluated compound displayed low inhibitory effect against *h*ERG channel (48 % at 1 μM) suggesting a moderate risk of evoking cardiovascular side effects.

To assess the potential risk of drug-drug interactions associated with compound **57**, a luminescence-based CYP3A4 P450–Glo assay was used [23]. Following 30 min of incubation, **57** exhibited significantly lower enzyme inhibition compared to reference compound ketoconazole (IC$_{50}$ = 12.2 μM *vs.* 0.127 μM, respectively) used as positive control (Fig. 16–SI).

2.7. Compound 57 is brain penetrant and exhibits good oral bioavailability

The preliminary pharmacokinetic profile of compound **57** was assessed in male Wistar rats after single intravenous (*iv*) or intragastric (*ig*) administration at the dose of 2 mg/kg or 10 mg/kg, respectively (Figs. 17A and 17B–SI). The evaluated compound displayed a good oral bioavailability of 57 % showing good exposure to the brain reaching the C$_{max}$ 78.9 ng/g in 120 min (Table 5) after oral administration. Moreover, compound **57** showed an adequate distribution in the systemic circulation with a brain/plasma ratio of 3.0 (*iv*) and 0.26 (*ig*).

Table 3
The antagonist properties, inverse agonist potency, efficacy estimates and binding data for selected compounds **56**, **57**, in-house derivatives PZ-1129 and PZ-1404, SB-269970 and lurasidone at h5-HT$_7$ receptor.

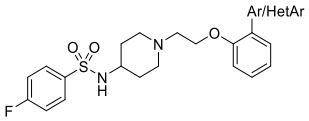

ID	Ar/HetAr	5-HT$_7$ receptor		
		K_i [nM] (pK_i ± SEM)[a]	K_B [nM] (pK_B ± SEM)[b]	EC$_{50}$ [nM] (pEC$_{50}$ ± SEM)[c]/ (-%SB-269970 ± SEM)
PZ-1129		7 (8.16 ± 0.06)	8.95 (8.05 ± 0.14)	13.7 (7.87 ± 0.05)/(-112 ± 2.0 %)
56		5 (8.31 ± 0.07)	0.84 (9.08 ± 0.16)	1.92 (8.72 ± 0.04)/(-93.4 ± 1.2 %)
57		5 (8.31 ± 0.06)	2.93 (8.53 ± 0.05)	2.93 (8.53 ± 0.03)/(-100.1 ± 1.1 %)
PZ-1404		10 (8.00 ± 0.05)	N.T.	27.7 (7.56 ± 0.04)/(-98.8 ± 1.5 %)
SB-269970		3 (8.52 ± 0.02)	0.81 (9.09 ± 0.05)	0.97 (9.02 ± 0.03)/(-100 %)
lurasidone		0.5[d] (9.30 ± 0.07)	N.T.	7.7 (8.11 ± 0.03)/(-101.2 ± 0.8 %)

[a] Mean K_i and pK_i values ± SEMs from at least three independent binding experiment in HEK293 cells for h5-HT$_7$,h5-HT$_{1A}$ and hD$_2$ receptors.
[b] Mean K_B and pK_B values ± SEMs from at least three independent experiments in HEK293T cells.
[c] Mean EC$_{50}$ and pEC$_{50}$ values ± SEM from at least three independent experiments in HEK293T cells.
[d] Data taken from Ref. [22]; N.T. not tested.

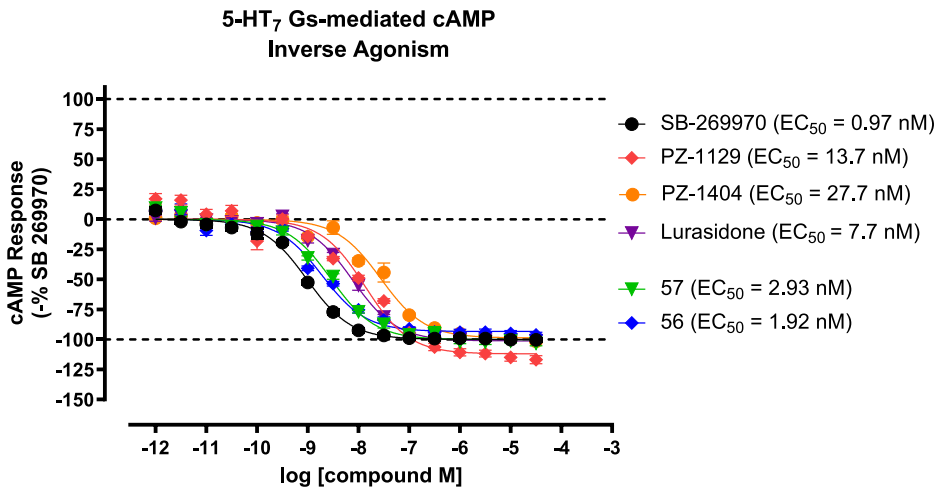

Fig. 3. Functional dose-response curve of cAMP inhibition indicative of inverse agonism at h5-HT$_7$ receptor for selected compounds **56**, **57**, PZ-1129, PZ-1404, SB-269970 and lurasidone in HEK293T cells. Data were obtained from at least three independent experiments performed in triplicate.

Table 4
The antagonist properties at h5-HT$_{1A}$ and D$_2$ receptors, and binding data for selected compounds **56**, **57**, PZ-1129, PZ-1404 and SB-269970 at h5-HT$_{1A}$, hD$_2$, h5-HT$_{2A}$ and h5-HT$_6$ receptors.

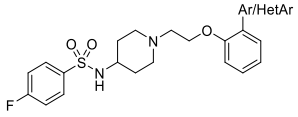

ID	Ar/HetAr	5-HT$_{1A}$ receptor		D$_2$ receptor		5-HT$_{2A}$ receptor	5-HT$_6$ receptor
		K_i [nM] (pK_i ± SEM)[a]	K_B [nM] (pK_B ± SEM)[b]	K_i [nM] (pK_i ± SEM)[a]	K_B [nM] (pK_B ± SEM)[c]	K_i [nM] (pK_i ± SEM)[a]	K_i [nM] (pK_i ± SEM)[a]
PZ-1129		159 (6.80 ± 0.07)	123 (6.91 ± 0.06)	24 (7.63 ± 0.07)	273 (6.56 ± 0.05)	113 (6.95 ± 0.06)	524 (6.28 ± 0.06)
56		99 (7.01 ± 0.07)	170 (6.77 ± 0.07)	899 (6.05 ± 0.07)	791 (6.10 ± 0.06)	191 (6.72 ± 0.06)	1650 (5.78 ± 0.06)
57		292 (6.54 ± 0.07)	197 (6.71 ± 0.05)	1004 (6.00 ± 0.06)	801 (6.09 ± 0.06)	435 (6.36 ± 0.06)	3282 (5.48 ± 0.07)
PZ-1404[d]		378 (6.42 ± 0.06)	78 (7.11 ± 0.06)	112 (6.95 ± 0.05)	255 (6.59 ± 0.07)	178 (6.75 ± 0.07)	490 (6.31 ± 0.06)
SB-269970		>1000 (<6)	N.A.	714 (6.15 ± 0.07)	232 (6.63 ± 0.07)	>1000 (<6)	>1000 (<6)

[a] Mean K_i and pK_i values ± SEMs from three independent binding experiment in HEK293 cells (for h5-HT$_7$, h5-HT$_{1A}$, h5-HT$_6$ and hD$_2$ receptors) or CHO cells (for h5-HT$_{2A}$ receptor).
[b] Mean K_B and pK_B values ± SEMs from three independent experiments in HEK293 cells with stable expression of h5-HT$_{1A}$ or hD$_2$ receptors.
[c] Compound 10 from Ref. [12]; N.A. = Not Active.

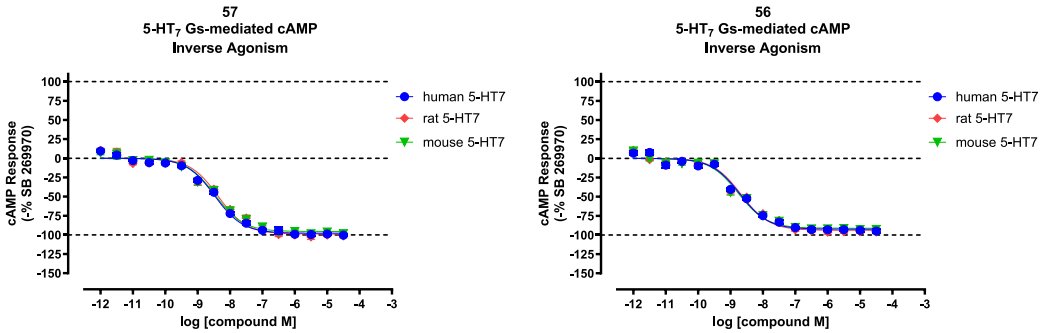

Fig. 4. Comparison of functional dose-response curves of cAMP inhibition indicative of inverse agonism at human, mouse and rat 5-HT$_7$ receptor for compounds **57** (left) and **56** (right) in HEK293T cells. Data were obtained from at least three independent experiments performed in triplicate.

Table 5
Pharmacokinetic parameters for compound **57** in rats.

Parameters	intravenous (*iv*)[b]		intragastric (*ig*)[c]	
	Plasma	Brain	Plasma	Brain
C0 [ng/mL]	599.9	NA	NA	NA
$AUC_{0\rightarrow t}$ [ng · min/mL] or [ng · min/g][a]	19552	59513	55900	14399
MRT [min]	55.1	89.9	56.6	117.9
$t_{0.5}$ [min]	NA	137.4	68.9	153.9
C_{max} [ng/mL] or [ng/g][a]	NA	527	1056.7	78.9
t_{max} [min]	NA	5	15	120
Cl [mL/min/kg]	84.6	NA	NA	NA
Vss [L/kg]	10	NA	NA	NA
F [%]	100		57.2	

C0 – initial concentration; AUC – area under the curve, MRT – mean residence time; $t_{0.5}$ – terminal half-life; C_{max} – maximum concentration; t_{max} – time to reach the maximum concentration; Cl – systemic clearance; Vss – volume of distribution at steady state F – bioavailability; NA – not available.

[a] Concentration in brain.

[b] Compound **57** in a dose of 2 mg/kg was administered intravenously (N = 28).

[c] Compound **57** in a dose of 10 mg/kg was administered via oral gavage (N = 28).

2.8. Compound 57 demonstrates antidepressant-like properties in FST

We assessed the ability of the most promising 5-HT_7 receptor inverse agonist **57** to produce antidepressant-like responses in FST. Compound **57** exerted antidepressant-like activity at the dose of 5 mg/kg (*ip*; $P < 0.05$ following ANOVA ($F(3.28) = 3.107$, $p = 0.042$)) by reducing the immobility time of mice of 25 % *vs.* control, while it was inactive at lower doses (1.25 and of 2.5 mg/kg). Compound **57** was more potent than the reference inverse agonist SB-269970 which displayed its antidepressant effect at 10 mg/kg, (*ip*; $P < 0.05$ following ANOVA: $F(3.29) = 3.550$, $p = 0.027$) decreasing the immobility time by 31 % *vs.* control (Fig. 5).

Effective doses of **57** and SB-269970 did not influence locomotor activity as compared with vehicle ($F(2.27) = 1.130$, $p = 0.338$). The counts/5 min were 159.8 ± 36.7, 95.5 ± 21.1 and 127.9 ± 30.1 for compound **57**, SB-269970 and vehicle, respectively.

The antidepressant-like property of **57** was also assessed in the tail suspension test (TST). Although it reduced the immobility as compared to controls, that effect was not statistically significant (Fig. 18–SI).

2.9. Compound 57 decreases 5-HT_7 receptor-mediated MMP-9 activity

We have previously reported that activation of 5-HT_7 receptor might induce depressive-like behavior in mice by stimulation of MMP-9, suggesting an involvement of the 5-HT_7 receptor/MMP-9 signaling module in the patho-mechanism of mood disorders [7]. Moreover, we demonstrated that both genetic and pharmacological blockade of the 5-HT_7 receptor constitutive activity (via 5-HT_7 receptor knockout in mice or administration of inverse agonist SB-269970), reduced the activation of MMP-9 in hippocampus. Thus, in a preliminary experiment on a restricted set of mice' hippocampi, we investigated the impact of compound **57** on MMP-9 activity in an *ex vivo* assay.

We found that administration of **57** at the dose active in FST (5 mg/kg, *ip*) significantly decreased the 5-HT_7 receptor-mediated MMP-9 activity in mouse hippocampi as compared to saline-treated animals (Fig. 6). Moreover, the observed effect was similar to that caused by SB-269970 (10 mg/kg, *ip*).

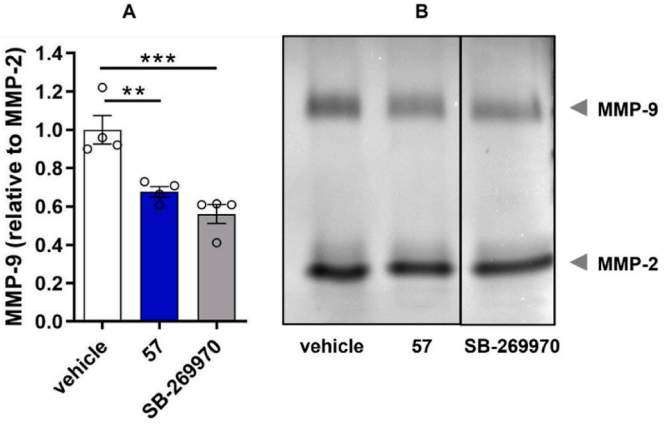

Fig. 6. A) Quantification of the MMP-9/MMP-2 activity ratio in the hippocampi of control, **57**- (5 mg/kg) and SB-269970- (10 mg/kg) treated mice; B) Representative gelatinase activity. Data are presented as the mean ± SEM of N = 4 animals per group. *p < 0.05; ***p < 0.001 *vs.* vehicle, Sidak's multiple comparisons test, following one-way ANOVA: $F(2.9) = 17.66$, $p = 0.0008$).

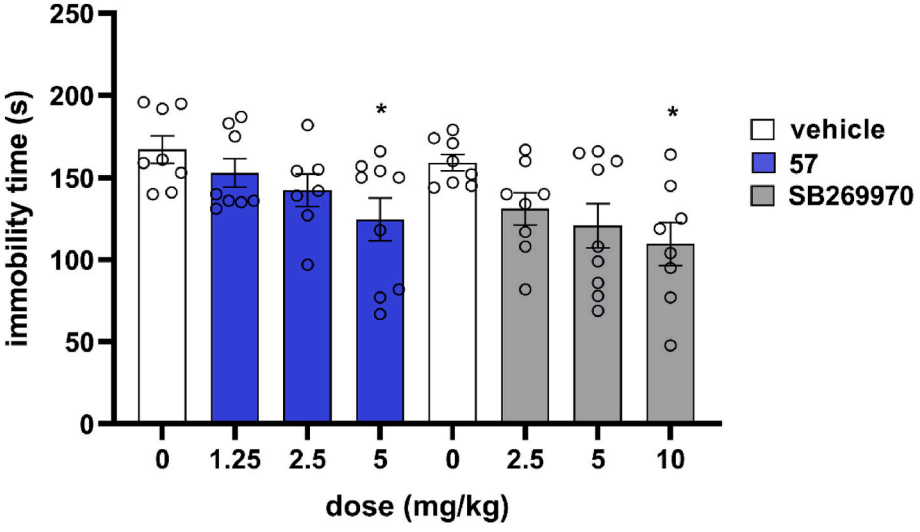

Fig. 5. Effect of compound **57** and reference SB-269970 (60 min and 30 min after *ip* administration, respectively) on immobility time of mice in the forced swim test. Data are presented as the mean ± SEM of N = 8–9 animals per group. *p < 0.05 compared to vehicle group, followed by Bonferroni's post *hoc test*.

2.10. Compound 57 reverses cognitive deficits induced by PCP in the NOR test

The cognitive properties of compound **57** were assessed in the NOR test. As expected, rats treated with vehicle, but not with phencyclidine (PCP, 5 mg/kg), spent significantly more time exploring the novel object than the familiar one (Fig. 19–SI). PCP-induced learning impairment was inhibited following *ip* administration of the compound **57** at a dose of 3 mg/kg, but not 1 mg/kg (Fig. 7). A similar effect was observed with 5-HT$_7$ receptor inverse agonist SB-269970, used as a positive control. Neither compound **57** nor SB-269970 affected object recognition in undisturbed vehicle conditions and did not affect rat's locomotor activity at Test 1 and 2 (Fig. 19–SI) and the time of object exploration at Test 1 (Fig. 20–SI).

3. Discussion

While majority of reported antagonists of 5-HT$_7$ receptor preferentially bind the receptor, they also show significant affinities for other serotonin and dopamine receptor subtypes, including 5-HT$_{1A}$ and D$_2$ receptors. This lack of selectivity complicates assignment of observed behavioral effects in animals specifically to the 5-HT$_7$ receptor. Additionally, pharmacokinetic limitations, such as low clearance and low bioavailability, may hinder the development of preclinical leads, as exemplified by SB-269970. Hence, we examined whether advancing the *in silico* simulations-driven structural diversity at the distal phenyl ring of the aryloxyl fragment of compound PZ-1129, a previously identified 5-HT$_7$ receptor ligand, could provide more selective and/or metabolically stable 5-HT$_7$ receptor inverse agonists.

The selection of compound PZ-1129 as a template for structural optimization was driven by two key factors. Firstly, previous SAR studies examining the replacement of the isopropyl group (present in PZ-766 and PZ-1404) with various alkyl, alkoxy or cycloalkyl substituents (e.g., methoxy, isopropoxy, cyclopentyl) failed to yield potent and selective 5-HT$_7$ receptor ligands with satisfactory metabolic stability. Secondly, the terminal phenyl moiety of the aryloxy fragment offers extensive opportunities for functionalization and bioisosteric replacement. The choice was further supported by the availability of diverse aryl and heteroaryl boronic acids and esters, enabling the diversification of the aryloxyl fragment through Suzuki coupling reactions.

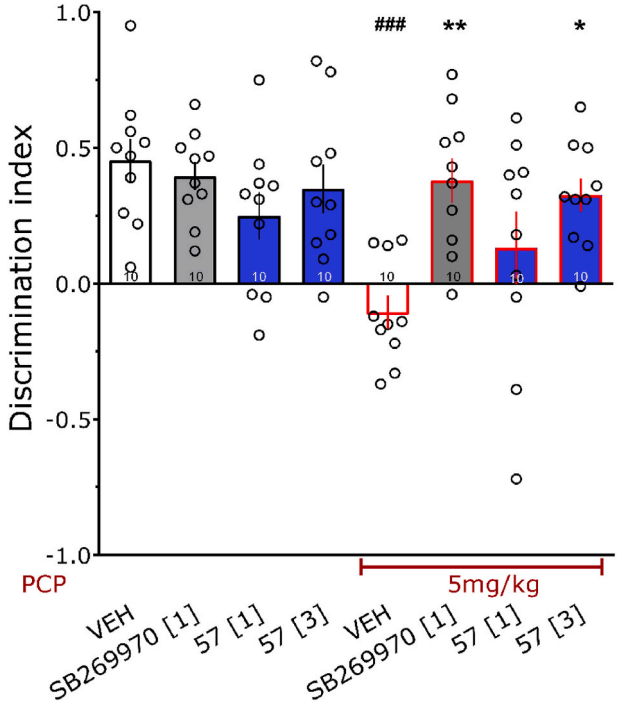

Fig. 7. Cognitive effects of compounds **57** and SB-269970 in vehicle undisturbed and PCP-disturbed conditions in the NOR test in rats. The data represent the means ± SEM of the discrimination index (DI) measured in 10 animals per group. Symbols: *p < 0.05 *vs.* vehicle-PCP group; **p < 0.01 *vs.* vehicle-PCP group, $^{###}$p < 0.001 *vs.* vehicle group; Tukey's multiple comparison post-hoc test following ANOVA: F(3.72) = 4.6979, P < 0.01. PCP (5 mg/kg) was administered *ip* 45min before Test 1 while compounds **57** and SB-269970 were given *ip* 30 min before PCP.

Accordingly, modifications at the distal phenyl moiety with neither electron-withdrawing nor electron-donating substituents improved selectivity for 5-HT$_{1A}$ and D$_2$ receptors (S < 20 and < 4, respectively), while an introduction of 3- or 4-pyridinyl moieties provided more potent, though still poorly selective 5-HT$_7$ receptor ligands (S < 9 for D$_2$ receptor). Moreover, replacing the phenyl ring with five-membered heteroaromatic moiety enhanced selectivity over D$_2$ receptor, identifying derivative **57** as potent and selective 5-HT$_7$ receptor inverse agonist. Importantly, **57** displayed similar selectivity over D$_2$ receptor to the reference SB-269970 (200- *vs.* 238-folds, respectively) but demonstrating two-fold higher metabolic stability (Cl$_{int}$ = 41.6 *vs.* 99.0 μL/min/mg, respectively) and more favorable bioavailability.

In addition, compound **57** showed no agonistic properties at 5-HT$_{1A}$ and D$_2$ receptors while displaying only low or marginal residual antagonistic activity at those targets (K$_B$ = 197 and 801 nM, respectively). Effects of compound **57** corroborated previous findings with selective 5-HT$_7$ receptor antagonists which produced antidepressant-like effect in FST in mice and reversed PCP-induced cognitive impairment in rats in the NOR task, without affecting the motor activity. Thus, these studies demonstrate that the bioisosteric replacement of phenyl ring or isopropyl moiety in the aryloxy fragment of parent compound PZ-1129 and PZ-1404 with *N*-methyl-3-pyrazolyl moiety, results in a more favorable *in vitro* and *in vivo* properties of compound **57** suggestive of more selective 5-HT$_7$ receptor inhibition. Present results also suggest contribution of the 5-HT$_7$ receptor-mediated inhibition of MMP-9 activity in mouse hippocampus to the antidepressant effect observed in rodents.

4. Conclusions

We developed a 27-member library of 4-fluorobenzenesulfonamide derivatives of 2-[(2-aryl/2-heteroaryl)phenoxy]ethyl-piperidines by combining conventional solution-phase method with a sustainable mechanochemical approach. The study expanded the chemical diversity of the *ortho* substituent at the aryloxy fragment of previously reported 5-HT$_7$ receptor antagonist PZ-1129 to investigate the effects of heterocyclic ring replacement for tuning receptor selectivity and metabolic stability.

Through structure-activity relationship studies supported by *in silico* simulations, we identified compound **57** as potent 5-HT$_7$ receptor ligand exhibiting high selectivity over 5-HT$_{1A}$ and D$_2$ receptors. Functional assays demonstrated that **57** acted as a strong inverse agonist by inhibiting constitutive Gs-mediated cAMP production showing potency comparable to that of the drug lurasidone (EC$_{50}$ = 2.93 *vs* 7.7 nM, respectively). Of note, its inhibitory potency was retained across human, mouse and rat 5-HT$_7$ receptor orthologs.

Pharmacokinetic profiling revealed that compound **57** possess good metabolic stability in RLM assay, favorable oral bioavailability and efficient blood-brain barrier penetration following *ig* administration in rats. In behavioral assays, **57** elicited antidepressant-like effects in FST in mice without impairing locomotor activity. At an active antidepressant dose, it also reduced 5-HT$_7$ receptor-mediated MMP-9 activity in the mouse hippocampus, mirroring the effects of the reference inverse agonist SB-269970.

Furthermore, compound **57** reversed the PCP-induced cognitive deficits in NOR test in rats, indicating its pro-cognitive properties.

Taken together, these findings support further investigations to

confirm the relevance of 5-HT_7 receptor/MMP-9 signaling pathway *in vivo* settings and to underscore the potential therapeutical application of **57** in treating affective disorders.

5. Experimental Section

5.1. Chemistry

5.1.1. General chemical methods

Organic solvents (from Merck and Thermofisher) were of reagent grade and were used without purification. Commercially available reagents were of the highest purity (from Aldrich, Fluorochem, Ambeed). In-solution reactions were carried out at ambient temperature, unless indicated otherwise. Mechanochemical reactions were carried out in a vibratory ball-mill Retsch MM400 operating at 30 Hz. The milling load was defined as the sum of the mass of the reactants per free volume in the jar and was equal to 45 or 90 mg/mL. All reactions using the vibratory ball mill were performed under air. Microwave-assisted reactions were conducted in Initiator $^+$ microwave synthesizer Biotage®. All workup and purification procedures were carried out with reagent-grade solvents under ambient atmosphere. Column chromatography was performed using silica gel Merck 60 (70–230 mesh ASTM).

^{1}H and ^{13}C NMR spectra were recorded on a JEOL JNM-ECZR500 RS1 (ECZR version) at 500 and 126 MHz, respectively, and were reported in ppm using deuterated solvent for calibration ($CDCl_3$, CD_3OD). The *J* values were reported in hertz (Hz), and the splitting patterns were designated as follows: br. s (broad singlet), s (singlet), d (doublet), t (triplet), dd (doublet of doublets), dt (doublet of triplets), td (triplet of doublets), ddd (doublet of doublet of doublets), ddt (doublet of doublet of triplets), m (multiplet).

Mass spectra were recorded on a UPLC/MS system consisting of a Waters ACQUITY UPLC (Waters Corporation, Milford, MA, USA) coupled to a Waters TQD mass spectrometer (electrospray ionization mode ESI-tandem quadrupole). Chromatographic separations were carried out using the Acquity UPLC BEH (bridged ethyl hybrid) 18 column × 2.1 mm × 100 mm, and 1.7 μm particle size, equipped with Acquity UPLC BEH C18 Van Guard precolumn; 2.1 mm × 5 mm, and 1.7 μm particle size. The column was maintained at 40 °C and eluted under gradient conditions from 95 % to 0 % of eluent A over 10 min, at a flow rate of 0.3 mL min^{-1}. Eluent A: water/formic acid (0.1 %, *v/v*), Eluent B: acetonitrile/formic acid (0.1 %, *v*/v). The UPLC/MS purity of all the final compounds was confirmed to be 95 % or higher.

Elemental analyses for C, H, N and S were carried out using the elemental Vario EI III Elemental Analyzer (Hanau, Germany). All values are given as percentages and were within ±0.4 % of the calculated values.

Compound selected for behavioral evaluation (**57**) was converted into the respective hydrochloride salt.

General synthetic procedures, as well as characterization data for representative final compounds, are summarized below. Characterization data for all intermediates and remaining final compounds, LC chromatograms, MS, ^{1}H and ^{13}C NMR spectra for final compounds are presented in the Supporting Information.

5.1.2. General procedure for alkylation of 2-iodophenol with 1,2-dibromoethane

A solution of 1,2-dibromoethane (51.23 g, 0.27 mol, 6 eq) in 20 mL of acetone was added dropwise into the mixture of 2-iodophenol (10 g, 0.045 mol, 1 eq), K_2CO_3 (15.7 g, 0.135 mol, 3 eq) in 50 mL of acetone. Subsequently, a catalytic amount of KI was added, and the resulting mixture was stirred at 60 °C for 48 h. After completion of the reaction, the inorganic residues were filtrated off, and the organic mixture was concentrated under vacuum. The obtained crude product was purified on silica gel with EtOAc/Hexane (0.5/9.5, *v/v*) as the eluting system.

5.1.3. General procedure for alkylation of 4-(N-Boc-amino)piperidine with 1-(2-bromoethoxy)2-iodobenzene

Bromine derivative **2** (1.04 g, 3.19 mmol, 1 eq) and 4-(Boc-*N*-amino) piperidine (0.64 g, 3.19 mmol, 1 eq) were introduced in two 35 mL PTFE jars (milling load 90 mg/mL) with one stainless steel ball (ϕ_{ball} = 1.5 cm), followed by the addition of K_2CO_3 (1.32 g, 9.56 mmol, 3 eq). The reaction was carried out for 60 min at rt. Then, the product was solubilized in EtOAc (60 mL), and the organic phase was washed with $KHSO_4$ aqueous solution at pH = 3.5 (3 × 20 mL) and saturated NaCl solution (1 × 20 mL), dried over Na_2SO_4, and finally filtered and concentrated under reduced pressure. To obtain the desired amount of product, the reaction was repeated three times (6 × 35 mL).

5.1.4. General procedure for palladium-catalyzed cross-coupling (Suzuki-Miyaura) reaction

In a microwave vial, a mixture of **3** (250 mg, 0.56 mmol, 1 eq), boronic acid derivative (1.2 eq) and tetrakis(triphenylphosphine)palladium(0) (33 mg, 0.028 mmol, 0.05 eq) was dissolved in 1,4-dioxane and saturated solution of K_2CO_3 (2/1, *v/v*), then heated at 140 °C for 2 h under microwave irradiation. After cooling to ambient temperature, the mixture was diluted with EtOAc, filtered through a Celite. Organic layer was washed three times with water (3 × 5 mL), brine (1 × 5 mL), dried over Na_2SO_4, filtered and concentrated under reduced pressure. The residue was purified on silica gel using CH_2Cl_2/MeOH as eluting system (the eluting system is indicated for each compound together with characterization data in the supporting information).

5.1.5. General procedure for one-pot two-step mechanochemical deprotection/sulfonylation of primary amine to obtain final compounds ***31–57***

Boc-protected intermediate (1 eq) was introduced into a 35 mL PTFE jar (milling load = 45 mg/mL) charged with a stainless steel ball (φ_{ball} = 1.5 cm) followed by addition of 6 M HCl solution in isopropanol (10 eq) in 3 portions after 10 min of milling. After completion of Boc removal, K_2CO_3 (25 eq) and 4-fluorobenzenesulfonyl chloride (1.1 eq) were added. The reaction was carried out for 5 min. The resulting powder from the jar was suspended in water and extracted with CH_2Cl_2 (3 × 10 mL) to yield final compound.

5.1.6. Characterization data for representative final compounds

5.1.6.1. *4-Fluoro-N-(1-{2-[(2′-fluoro-[1,1′-biphenyl]-2-yl)oxy]ethyl} piperidin-4-yl)benzene sulfonamide (**31**).*

Colorless oil, 127 mg (yield 87 %), UPLC/MS purity = 100 %, t_R = 5.49 min, $C_{25}H_{26}F_2N_2O_3S$, MW 472.55, Monoisotopic Mass 472.16, $[M+H]^+$ 473.1. ^{1}H NMR (500 MHz, $CDCl_3$) δ ppm 1.44–1.55 (m, 2H), 1.67 (d, J = 12.7 Hz, 2H), 2.02–2.19 (m, 2H), 2.69–2.81 (m, 4H), 3.11 (s, 1H), 4.10 (t, J = 5.4 Hz, 2H), 4.82 (br. s, 1H), 6.94 (dd, J = 8.3, 1.1 Hz, 1H), 7.02–7.09 (m, 2H), 7.14 (td, J = 7.5, 1.2 Hz, 1H), 7.16–7.21 (m, 2H), 7.24–7.27 (m, 1H), 7.27–7.32 (m, 2H), 7.34 (ddd, 8.3, 7.5, 1.8 Hz, 1H), 7.87–7.93 (m, 2H). ^{13}C NMR (126 MHz, $CDCl_3$) δ ppm 32.8, 50.5, 52.2, 56.7, 66.8, 112.2, 115.3 (d, $J_{C\text{-}F}$ = 22.5 Hz), 116.4 (d, $J_{C\text{-}F}$ = 22.6 Hz), 121.0, 123.8 (d, $J_{C\text{-}F}$ = 3.6 Hz), 125.5, 126.4 (d, $J_{C\text{-}F}$ = 16.2 Hz), 129.0 (d, $J_{C\text{-}F}$ = 8.0 Hz), 129.5, 129.7 (d, $J_{C\text{-}F}$ = 9.2 Hz), 131.4, 132.1 (d, $J_{C\text{-}F}$ = 3.8 Hz), 137.5 (d, $J_{C\text{-}F}$ = 3.1 Hz), 156.1, 160.1 (d, $J_{C\text{-}F}$ = 247.1 Hz), 165.1 (d, $J_{C\text{-}F}$ = 254.5 Hz).

5.1.6.2. *4-Fluoro-N-(1-{2-[(3′-methoxy-[1,1′-biphenyl]-2-yl)oxy]ethy} piperidin-4-yl)benzene sulfonamide (**35**).*

White solid, 123 mg (yield 82 %), UPLC/MS purity = 95 %, t_R = 5.47 min, $C_{26}H_{29}FN_2O_4S$, MW 484.59, Monoisotopic Mass 484.18, $[M+H]^+$ 485.0. ^{1}H NMR (500 MHz, $CDCl_3$) δ ppm 1.44–1.54 (m, 2H), 1.65–1.74 (m, 2H), 2.06–2.17 (m, 2H), 2.69–2.82 (m, 4H), 3.08–3.16 (m, 1H), 3.81 (s, 3H), 4.06 (t, J = 5.5 Hz, 2H), 4.81 (br. s, 1H), 6.84 (ddd, J = 8.3, 2.6, 1.0 Hz, 1H), 6.93 (dd, J = 8.3, 1.1 Hz, 1H), 7.03 (td, J = 7.5, 1.1 Hz, 1H), 7.05–7.08 (m, 2H), 7.16–7.21 (m, 2H), 7.26–7.33 (m, 3H), 7.87–7.92 (m, 2H). ^{13}C NMR

(126 MHz, $CDCl_3$) δ ppm 32.7, 50.4, 52.3, 55.4, 56.8, 66.6, 112.4, 112.9, 114.7, 115.6, 116.5 (d, J_{C-F} = 22.4 Hz), 121.4, 122.3, 128.9 (d, J_{C-F} = 3.8 Hz), 129.7 (d, J_{C-F} = 9.4 Hz), 131.0, 131.1, 137.5, 140.0, 155.6, 159.3, 165.1 (d, J_{C-F} = 254.7 Hz).

*5.1.6.3. 4-Fluoro-N-(1-{2-[(4′-methoxy-[1,1′-biphenyl]-2-yl)oxy]ethy} piperidin-4-yl)benzene sulfonamide (**38**).* Yellow solid, 124 mg (yield 83 %), UPLC/MS purity = 100 % t_R = 5.35 min; $C_{26}H_{29}FN_2O_4S$, MW 484.59, Monoisotopic Mass 484.18, $[M+H]^+$ 485.0. ^{1}H NMR (500 MHz, $CDCl_3$) δ ppm 1.40–1.50 (m, 2H), 1.66–1.73 (m, 2H), 2.03–2.13 (m, 2H), 2.68 (t, J = 5.6 Hz, 2H), 2.71–2.76 (m, 2H), 3.06–3.18 (m, 1H), 3.84 (s, 3H), 4.02 (t, J = 5.6 Hz, 2H), 5.04–5.25 (m, 1H), 6.92 (td, J =7.1, 1.6 Hz, 3H), 7.01 (td, J = 7.5, 1.1 Hz, 1H), 7.14–7.22 (m, 2H), 7.23–7.27 (m, 1H), 7.29 (dd, J =7.6, 1.8 Hz, 1H), 7.42–7.50 (m, 2H), 7.82–7.98 (m, 2H). ^{13}C NMR (126 MHz, $CDCl_3$) δ ppm 32.9, 50.6, 52.3, 55.4, 56.9, 66.7, 112.8, 113.4, 114.6, 116.4 (d, J_{C-F} = 22.6 Hz), 121.3, 128.2, 129.5, 129.7 (d, J_{C-F} = 9.1 Hz), 130.7, 130.8, 130.9, 137.5 (d, J_{C-F} = 3.3 Hz), 155.7, 158.7, 165.0 (d, J_{C-F} = 254.6 Hz).

*5.1.6.4. 4-Fluoro-N-(1-{2-[2-(6-methoxypyridin-3-yl)phenoxy]ethyl} piperidin-4-yl)benzene sulfonamide (**44**).* White solid, 117 mg (yield 78 %), UPLC/MS purity = 100 %, t_R = 5.01 min; $C_{25}H_{28}FN_3O_4S$, MW 485.57, Monoisotopic Mass 485.18, $[M+H]^+$ 486.3. ^{1}H NMR (500 MHz, $CDCl_3$) δ ppm 1.47–1.87 (m, 4H), 2.17 (s, 2H), 2.69–2.91 (m, 4H), 3.16 (s, 1H), 3.96 (s, 3H), 4.07–4.15 (m, 2H), 4.75–4.97 (m, 1H), 6.75 (dd, J =8.5, 0.8 Hz, 1H), 6.94 (dd, J =8.2, 1.1 Hz, 1H), 7.04 (td, J =7.5, 1.1 Hz, 1H), 7.16–7.22 (m, 2H), 7.27–7.32 (m, 2H), 7.75 (dd, J =8.6, 2.4 Hz, 1H), 7.87–7.92 (m, 2H), 8.28 (dd, J =2.4, 0.7 Hz, 1H). ^{13}C NMR (126 MHz, $CDCl_3$) δ ppm 32.9, 52.4, 53.6, 56.9, 66.6, 109.8, 112.6, 116.5 (d, J_{C-F} = 22.5 Hz), 121.4, 127.4, 127.5, 129.0, 129.7 (d, J_{C-F} = 9.3 Hz), 130.5, 137.5 (d, J_{C-F} = 3.4 Hz), 140.2, 147.1, 155.8, 163.1, 165.1 (d, J_{C-F} = 254.6 Hz).

*5.1.6.5. 4-Fluoro-N-(1-{2-[2-(5-fluoropyridin-3-yl)phenoxy]ethyl}piperidin-4-yl)benzene sulfonamide (**48**).* Yellow solid, 136 mg (yield 93 %), UPLC/MS purity = 98 % t_R = 4.49 min; $C_{24}H_{25}F_2N_3O_3S$, MW 473.54, Monoisotopic Mass 473.16, $[M+H]^+$ 474.2. ^{1}H NMR (500 MHz, $CDCl_3$) δ ppm 1.55–1.65 (m, 2H), 1.77–1.85 (m, 2H), 2.18 (t, J =10.1 Hz, 2H), 2.77 (t, J =5.4 Hz, 2H), 2.82–2.92 (m, 2H), 3.23 (dt, J =8.5, 4.1 Hz, 1H), 4.18 (dt, J = 24.9, 5.4 Hz, 2H), 5.56 (d, J =7.7 Hz, 1H), 7.05 (dd, J =8.3, 1.1 Hz, 1H), 7.15 (dd, J =7.5, 1.1 Hz, 1H), 7.26 (ddt, J =9.8, 8.1, 2.6 Hz, 2H), 7.38–7.51 (m, 2H), 7.80 (ddd, J =9.9, 2.8, 1.7 Hz, 1H), 7.94–8.03 (m, 2H), 8.42–8.54 (m, 1H), 8.59–8.78 (m, 1H). ^{13}C NMR (126 MHz, $CDCl_3$) δ ppm 32.9, 50.6, 52.4, 56.8, 66.4, 112.5, 116.4 (d, J_{C-F} = 22.5 Hz), 121.5, 124.0 (d, J_{C-F} = 18.5 Hz), 125.6, 128.7 (d, J_{C-F} = 102.1 Hz), 129.7 (d, J_{C-F} = 9.4 Hz), 130.4 (d, J_{C-F} = 51.5 Hz), 135.8, 136.0, 137.6 (d, J_{C-F} = 3.6 Hz), 146.1 (d, J_{C-F} = 3.8 Hz), 155.7, 159.2 (d, J_{C-F} = 255.0 Hz), 165.0 (d, J_{C-F} = 254.5 Hz).

*5.1.6.6. 4-Fluoro-N-(1-{2-[2-(furan-3-yl)phenoxy]ethyl}piperidin-4-yl) benzenesulfonamide (**54**).* Yellow solid, 111 mg (yield 80 %), UPLC/MS purity = 97 %, t_R = 5.06 min; $C_{23}H_{25}FN_2O_4S$, MW 444.52, Monoisotopic Mass 444.15, $[M+H]^+$ 445.3. ^{1}H NMR (500 MHz, $CDCl_3$) δ ppm 1.50–1.68 (m, 2H), 1.70–1.90 (m, 2H), 2.11–2.34 (m, 2H), 2.71–3.08 (m, 4H), 3.22 (s, 1H), 4.17 (s, 2H), 4.70 (br. s, 1H), 6.79 (dd, J =1.9, 0.8 Hz, 1H), 6.92 (dd, J =8.3, 1.1 Hz, 1H), 7.00 (td, J =7.5, 1.1 Hz, 1H), 7.15–7.23 (m, 3H), 7.44 (t, J =1.7 Hz, 1H), 7.49 (dd, J =7.6, 1.7 Hz, 1H), 7.87–7.93 (m, 2H), 8.16 (s, 1H). ^{13}C NMR (126 MHz, $CDCl_3$) δ ppm 33.0, 50.8, 52.3, 57.1, 65.8, 109.4, 112.1, 116.5 (d, J_{C-F} = 22.6 Hz), 121.2, 121.6, 121.7, 127.8, 128.0, 129.7 (d, J_{C-F} = 9.3 Hz), 137.4, 142.3 (d, J_{C-F} = 8.2 Hz), 155.6, 165.1 (d, J_{C-F} = 254.7 Hz).

*5.1.6.7. 4-Fluoro-N-(1-{2-[2-(1-methyl-1H-pyrazol-4-yl)phenoxy]ethyl} piperidin-4-yl) benzenesulfonamide hydrochloride (**57**).* Compound was dissolved in anhydrous ethanol and treated with 1.25 M methanolic HCl solution at 0 °C. After 2 h, the precipitate was filtered to yield the final compound as hydrochloride salt. White solid, 130 mg (yield 88 %, two steps), UPLC/MS purity = 100 %, t_R = 5.13 min, $C_{23}H_{27}FN_4O_3S$·HCl, MW 495.01, Monoisotopic Mass 458.18, $[M+H]^+$ 459.4. ^{1}H NMR (500 MHz, CD_3OD) δ ppm 1.74–2.08 (m, 4H), 3.14 (br s, 1H), 3.31–3.48 (m, 2H), 3.51–3.85 (m, 4H), 4.07–4.18 (m, 3H), 4.42–4.56 (m, 2H), 7.06–7.19 (m, 2H), 7.23–7.39 (m, 3H), 7.55 (br d, J =7.3 Hz, 1H), 7.87–7.95 (m, 2H), 8.32–8.55 (m, 2H). ^{13}C NMR (126 MHz, CD_3OD) δ ppm 29.9, 37.6, 48.6, 52.3, 55.6, 63.1, 112.7, 116.0 (d, J_{C-F} = 7.8 Hz), 119.1, 119.7, 122.1, 128.6 (d, J_{C-F} = 20.8 Hz), 129.1, 129.3, 129.6 (d, J_{C-F} = 9.5 Hz), 129.9 (d, J_{C-F} = 9.5 Hz), 133.4, 133.7, 134.5, 134.7, 137.8 (d, J_{C-F} = 3.0 Hz), 154.3, 165.2 (d, J_{C-F} = 271.9 Hz). Anal. calcd for $C_{23}H_{27}FN_4O_3S$·HCl, C: 55.81 %, H: 5.70 %, N: 11.32 %, S: 6.47 %; Found C: 55.41 %, H: 5.98 %, N: 10.98 %, S: 6.70 %.

5.2. In silico modelling

The three-dimensional models of 5-HT_7 (fetched form GPCRdb), 5-HT_{1A} (PDB ID: 7E2Z) and D_2 receptors (PDB ID: 7JVR) were prepared using the Protein Preparation Wizard tool in Maestro (Schrödinger Release 2024-3, Schrödinger, New York, NY, USA) [24]. Initial pre-processing steps included removing the co-crystalized inhibitor. Bond orders were then assigned, hydrogen atoms added, and optimization of H-bond assignments. For all compounds analyzed within this study, ionization states were generated at pH = 7.4 using Epik software (Release 2024-3, Schrödinger, LLC, New York, NY, 2024) [25]. Ligprep software (Release 2024-3, Schrödinger, LLC, New York, NY, 2024), under the default settings: generation of only one low energy ring conformation per ligand, and force field used OPLS2005, was applied for the generation of 3D structures. All receptor structures have been centered on D3.32 residue. Grid box size was set to 25 × 25 × 25 Å. All the docking calculations were run in Glide software (Release 2024-3, Schrödinger, LLC, New York, NY, 2024) at the SP level under the default settings (performing post-docking optimization, up to 100 steps during energy minimization, penalizing nonplanar conformation of amides, sampling ring conformations with energy window equal to 2.5 kcal/mol and sampling nitrogen inversion) generating 10 poses per ligand [26,27].

5.3. Molecular dynamics simulations

A 200 ns-long molecular dynamics simulations were performed using Desmond software from Schrodinger Suite (Release 2025-2, Desmond Molecular Dynamics System, D. E. Shaw Research, New York, NY, 2024). Each ligand−protein complex was placed in a two-layer POPC membrane (300 K). Next, the system was solvated (the TIP3P potential was used, boxtype - orthorhombic; box size - buffer of 10 Å from the solute), all atoms were parametrized (the OPLS_2005 force field was employed), and the ionic strength was added (0.15 M concentration of NaCl).

5.4. Radioligand binding experiments

HEK293 cells stably expressing human 5-HT_{1A}, 5-HT_6, 5-HT_{7b} and D_{2L} receptors (prepared using Lipofectamine 2000) or CHO–K1 cells transfected with a plasmid encoding the human serotonin 5-HT_{2A} receptor (PerkinElmer) were maintained at 37 °C in a humidified atmosphere containing 5 % CO_2. The cells were cultured in Dulbecco's Modified Eagle's Medium supplemented with 10 % dialyzed fetal bovine serum and 500 μg/mL G418 sulfate. For membrane preparation, cells were cultured in 150 cm^2 flasks, until 90 % confluence, washed twice with pre-warmed phosphate buffered saline (PBS) to 37 °C and centrifuged at 200×g in PBS with 0.1 mM EDTA and 1 mM dithiothreitol. The resulting cell pellets were stored at −80 °C until the membrane isolation. Before membrane isolation, the pellets were thawed and then homogenized in 10 vol of assay buffer using an Ultra Turrax tissue homogenizer

and centrifuged twice at 35,000×*g* for 15 min at 4 °C, with a 15 min incubation at 37 °C between the centrifugations. The composition of the assay buffers was optimized to maximize the signal window based on previous studies [28,29]. The assays were then conducted in 96-well plates with a total volume of 200 μL per well, incubated at 37 °C for 1 h, except for 5-HT_{1A} and 5-HT_{2A} receptor assays, which were incubated at room temperature and 27 °C, respectively. The equilibrium was halted by swift filtration using GF/C UniFilter plates (PerkinElmer, USA) with a 96-well cell harvester. The radioactivity retained on the filters was measured using a Microbeta plate reader (PerkinElmer, USA). For displacement studies, the assay samples included radioligands (PerkinElmer, USA): 2.5 nM [^{3}H]-8-OH-DPAT (135.2 Ci/mmol) for 5-HT_{1A} receptor; 1 nM [^{3}H]-ketanserin (53.4 Ci/mmol) for 5-HT_{2A} receptor; 2 nM [^{3}H]-LSD (83.6 Ci/mmol) for 5-HT_6 receptor; 0.8 nM [^{3}H]-5-CT (39.2 Ci/mmol) for 5-HT_7 receptor or 2.5 nM [^{3}H]-raclopride (76.0 Ci/mmol) for D_{2L} receptor. Non-specific binding was defined in the presence of 10 μM of 5-HT in 5-HT_{1A} receptor and 5-HT_7 receptor binding experiments, while 20 μM of mianserin, 10 μM of methiothepine or 10 μM of haloperidol were used in 5-HT_{2A}, 5-HT_6 and D_{2L} receptor assays, respectively. Each compound was tested at seven concentrations ranging from 10^{-10} to 10^{-4} M. The inhibition constants (K_i) were calculated using the Cheng-Prusoff equation [30].

5.5. In vitro metabolic stability study

The metabolic stability of compounds **54**, **56**, **57**, PZ-1129, PZ-1404 and SB-267790 was performed according to the previously published procedures [31,32]. Solution of the tested compounds (final concentration: 10 μM) were pre-incubated in a phosphate buffer (pH = 7.4) containing rat liver microsomes (RLMs, microsomes from male rat liver, pooled, 0.5 mg/mL, Merck/Millipore Sigma, Darmstadt, Germany) for 10 min at 37 °C. The reaction was initiated by adding the NADPH-regenerating system (consisting of $NADP^+$, glucose-6-phosphate and glucose-6-phosphate dehydrogenase in 100 mM phosphate buffer, pH 7.4; all from Sigma Aldrich), followed by incubation for 0, 30, and 60 min at 37 °C. Control samples were prepared by replacing the NADPH-regenerating system with phosphate buffer. The reactions were stopped by adding an ice-cold methanol solution of internal standard (pentoxifylline, 100 nM). The samples were then centrifuged, and the supernatants were analyzed by UPLC/MS.

Mass spectra were recorded on a UPLC/MS system consisting of a Waters ACQUITY UPLC (Waters Corporation, Milford, MA, USA) coupled to a Waters TQD mass spectrometer (electrospray ionization mode ESI-tandem quadrupole). Chromatographic separations were carried out using the Acquity UPLC BEH (bridged ethyl hybrid) 18 column × 2.1 mm × 100 mm, and 1.7 μm particle size, equipped with Acquity UPLC BEH C18 Van Guard precolumn; 2.1 mm × 5 mm, and 1.7 μm particle size. The column was maintained at 40 °C and eluted under gradient conditions from 95 % to 0 % of eluent A over 10 min, at a flow rate of 0.3 mL min^{-1}. Eluent A: water/formic acid (0.1 %, *v/v*), Eluent B: acetonitrile/formic acid (0.1 %, *v*/v). The injection volume was 10 μL, and the total time of analysis was 13 min.

All experiments were conducted in duplicates. The half-life time ($t_{1/2}$) of the compounds was determined from the slope of the line on Ln (% remaining of parent compounds) *vs*. time plots. The intrinsic clearance (Cl_{int}) was calculated using the equation: Cl_{int} = [volume of incubation (μL)/amount of protein (mg) × 0.693]/$t_{1/2}$. The assay performance was confirmed by using imipramine, an extensive metabolized drug, as reference.

5.6. Assessment of the impact of tested compounds on Gs activity

The inverse agonist properties of compounds **56**, **57**, PZ-1129, PZ-1404, SB-269970 and lurasidone at 5-HT_7 receptor-dependent Gs signaling pathway were assessed by measuring the inhibition of cAMP production in transiently transfected HEK293T cells expressing human, mouse or rat 5-HT_7 receptors and GloSensor-22F cAMP sensor following previously described procedures [33]. HEK293T cells (ATCC CRL-11268; mycoplasma-free) were co-transfected in 1:1 ratio with GloSensor-22F plasmid (Promega). Cells were transfected in 10 % dFBS, and next day cells were plated into poly-L-lysine-coated 384-well white assay plates (Grenier Bio-One) at a density of approximately 15,000 cells per well. After approximately 48 h post-transfection, plates were decanted and 20 μL per well of drug buffer (1 × HBSS, 20 mM HEPES, pH = 7.4) containing 4 mM D-luciferin (sodium salt; GoldBio) was added using a Multidrop (ThermoFisher Scientific). Cells were allowed to equilibrate for approximately 15 min at room temperature and then challenged with serial dilution of tested compounds (diluted in drug buffer containing 0.3 % BSA and 0.03 % ascorbic acid), dispensed by a FLIPR^{TETRA}. Next, cells were incubated for exactly 30 min at room temperature to assess endogenous cAMP accumulation by reading plates for luminescence (LCPS) on a Microbeta Trilux (PerkinElmer). For competition experiments to calculate antagonist affinities (K_B values), 5-HT (10 nM) was applied in presence of several concentrations of competitor to obtain IC_{50} estimates. K_B values were calculated from the Cheng–Prusoff equation specific for the analysis of functional inhibition curves: $K_B = IC_{50}/(1+A/EC_{50})$ where A is the agonist concentration, IC_{50} is the concentration of the antagonist producing a 50 % reduction in the response to the agonist, and EC_{50} is the agonist concentration which causes 50 % of the maximal response [34]. In case of 5-HT as positive control, EC_{50} = 2.07 nM.

5.7. Assessment of agonist/antagonist properties at 5-HT_{1A} and D_2 receptors in cAMP-based assay

HEK293 cell line with stable expression of human 5-HT_{1A} or D_2 receptors (prepared with the use of Lipofectamine 2000) was maintained at 37 °C in a humidified atmosphere with 5 % CO_2 and was grown in Dulbeco's Modifier Eagle Medium containing 10 % dialysed fetal bovine serum and 500 μg/ml G418 sulfate. For functional experiments, cells were subcultured in 25 cm^2 flasks, grown to 90 % confluence, washed twice with prewarmed to 37 °C phosphate buffered saline (PBS) and were centrifuged for 5 min (160×*g*). The supernatant was aspirated, the cell pellet was resuspended in stimulation buffer (1 × HBSS, 5 mM HEPES, 0.5 mM IBMX, 0.1 % BSA). The functional properties of compounds were evaluated using LANCE Ultra cAMP detection kit (PerkinElmer). Cells were stimulated with 1 μM of forskolin (EC_{90}). Each compound was tested in triplicate at 8 concentrations. For quantification of cAMP levels, cells (5 μl) with stable expression of 5-HT_{1A} receptor, were incubated with 5 μl mixture of compounds (tested ligand and forskolin with or without 1 μM (*R*)-(+)-8-OH-DPAT for agonist and antagonist mode, respectively) for 30 min at room temperature in 384-well white opaque microtiter plate (PerkinElmer). Alternatively, cells (5 μl) with stable expression of D_2 receptor, were incubated with 5 μl mixture of compounds (tested ligand and forskolin with or without 100 nM quinpirole for agonist and antagonist mode, respectively) for 30 min at room temperature in 384-well white opaque microtiter plate (PerkinElmer). After incubation, the reaction was stopped and cells were lysed by the addition of 10 μl working solution (5 μl Eu-cAMP and 5 μl ULight-*anti*-cAMP). The assay plate was incubated for 1 h at room temperature. Time-resolved fluorescence resonance energy transfer (TR-FRET) signal was detected by an Infinite M1000 Pro (Tecan) using instrument settings from LANCE Ultra cAMP detection kit manual.

5.8. Assessment of the impact of tested compounds on CYP3A4 isoform activity

A luminescence-based CYP3A4 P450-Glo™ assay kit (Promega, Madison, WI, USA) was used to evaluate the impact of the tested compound on cytochrome P450 isoform 3A4 activity. The assay was conducted according to the manufacturer's protocol and in accordance with previously described methods [23]. Each experiment was performed in

triplicate, with each sample run in duplicate. Luminescence signals were measured using a Spark microplate reader (Tecan, Männedorf, Switzerland) and converted to percent CYP3A4 activity relative to the following controls: (i) complete inhibition using the reference inhibitor ketoconazole (10 μM); and (ii) baseline activity with the solvent control (0.2 % DMSO). Sigmoidal dose-response curves were fitted to the resulting data using GraphPad Prism software (version 8.4.3; GraphPad Software, San Diego, CA, USA) and used to calculate IC_{50} values.

5.9. In vivo pharmacokinetic study

A group of 56 male, 8-week-old, Wistar strain outbred rats weighing between 200 and 220 g each were purchased from the Animal House at the Faculty of Pharmacy, Jagiellonian University Medical College, Krakow (Poland) and housed in standard polycarbonate cages, in groups of four animals per cage. Environmental conditions during the study were constant: relative humidity 50−60 %, temperature 22 ± 2 °C, normal 12 h light−dark cycle (7 a.m.–7 p.m. light). Standard rodent chow and water were available ad libitum. Compounds **57** were dissolved in a mixture of 5 % ethanol, 10 % Koliphor and 85 % distilled water and administered intravenous (at a dose of 2 mg/kg) or by intragastric gavage (at a dose of 10 mg/kg), and the animals were sacrificed at specific time-points: 0 min, pre-dose (n = 4), 5 min (n = 4), 15 min (n = 4), 30 min (n = 4), 60 min (n = 4), 120 min (n = 4), 240 min (n = 4), after administration. Animals were deeply anaesthetized by *ip* injections of 50 mg/kg ketamine plus 8 mg/kg xylazine before sacrifice. First, the blood was collected into heparinized tubes, and the blood samples were centrifuged at 1000g for 10 min to obtain plasma. Following the animals' euthanasia, the whole brain was collected. The plasma and brain samples were immediately frozen at −80 °C for future analysis. All experimental procedures were carried out in accordance with EU Directive 2010/63/EU and approved by the I Local Ethics Committee for Experiments on Animals of the Jagiellonian University in Krakow, Poland (No. 456/2020). Detailed experimental procedures are presented in the Supporting Information.

5.10. In vivo pharmacological evaluation

5.10.1. Forced swim test in mice

The experiment was carried out according to the method described by Porsolt et al. [35]. Adult male mice (Swiss albino, 22–26 g) purchased from a licensed breeder Staniszewska (Ilkowice, Poland) were used in the experiments. The animals were kept in groups of ten in Makrolon type 3 cages (dimensions 26.5 × 15 × 42 cm) in environmentally controlled rooms (ambient temperature 22 ± 2 °C; relative humidity 50–60 %; 12:12 light: dark cycle, lights on at 7:00). Mice were allowed to acclimate to the environment for one week prior to the start of the experiments. Standard pellet food and filtered water were freely available. All experimental procedures were approved by the I Local Ethics Commission at Jagiellonian University in Krakow (No. 83/2018). The experiment was carried out in the light phase between 09.00 and 14.00. Each experimental group consisted of 8–9 animals/dose. The animals were used only once. The experiments were carried out by an observer unaware of the treatment administered. Compound **57** were solubilized in a mixture of 5 % ethanol, 10 % koliphor and 85 % distilled water. Koliphor solution (Sigma-Aldrich, Germany) was used as a control. Both compounds were administered intraperitoneally (*ip*) at a volume of 10 mL/kg, 60 min (**57**) or 30 min (SB-269970) prior to the test. Control animals received a vehicle injection. Results are presented as means ± standard error of the mean (SEM). Comparison between experimental and control groups was performed by one-way ANOVA, followed by Bonferroni's post-hoc test. Differences in means were considered statistically significant when $p < 0.05$.

5.10.2. Novel object recognition test

The protocol was performed according to described earlier procedure [36], adapted from the original work of Ennaceur and Delacour [37]. 80 Male Sprague–Dawley rats (Charles River, Germany) weighing ~250 g at the arrival were housed in the standard laboratory cages, under standard colony A/C controlled conditions: room temperature 21 ± 2 °C, humidity (40–50 %), 12-h light/dark cycle (lights on: 06:00) with ad libitum access to food and water. Rats were allowed to acclimatize for at least 7 days before the start of the experimental procedure. During this week animals were handled for at least 3 times. Behavioral testing was carried out during the light phase of the light/-dark cycle. PCP (Sigma-Aldrich, Germany) was diluted in distilled water, 0,9 % NaCl was used as a control, compounds were administrated in a volume of 1 mL/kg. SB-269970 (Tocris, Bristol, UK) was diluted in distilled water, whereas compound **57** as hydrochloride salt was diluted in a mixture of 5 % ethanol, 10 % koliphor and 85 % distilled water. Koliphor solution (Sigma-Aldrich, Germany) was used as a control. All compounds were administrated in a volume of 1 mL/kg. All the experiments were carried out following the NIH Guide for the Care and Use of Laboratory Animals and were approved by the Ethics Committee for Animal Experiments, Maj Institute of Pharmacology (No. 214/2020). Detailed experimental procedures are reported at the Supporting Information.

5.11. Impact of compound 57 on MMP-9 activity in ex vivo model

Adult male mice (Swiss albino, 22–26 g) purchased from a licensed breeder Staniszewska (Ilkowice, Poland) were used in the experiments. The animals were kept in groups of ten in Makrolon type 3 cages (dimensions 26.5 × 15 × 42 cm) in environmentally controlled rooms (ambient temperature 22 ± 2 °C; relative humidity 50–60 %; 12:12 light: dark cycle, lights on at 7:00). Mice were allowed to acclimate to the environment for one week prior to the start of the experiments. Standard pellet food and filtered water were freely available. All experimental procedures were approved by the I Local Ethics Commission at Jagiellonian University in Krakow (No. 579/2021). The experiment was carried out in the light phase between 09.00 and 14.00. Each experimental group consisted of 8–9 animals/dose. The animals were used only once. The experiments were carried out by an observer unaware of the treatment administered. Compound **57** and SB-269970 were solubilized in a mixture of 5 % ethanol, 10 % koliphor and 85 % distilled water. Koliphor solution (Sigma-Aldrich, Germany) was used as a control. Both compounds were administered intraperitoneally (*ip*) at a volume of 10 mL/kg, 60 min (**57**) or 30 min (SB-269970) before sacrifice. MMPs were extracted from brain tissue via affinity chromatography using gelatin-Sepharose 4B (GE Healthcare) as previously described with minor modifications [7]. The tissues were homogenized in a working buffer consisting of 50 mM Tris-HCl, pH 7.5, 150 mM NaCl, 5 mM $CaCl_2$, and 1 % Triton X-100 containing 0.02 % NaN_3. The homogenates were centrifuged for 15 min at 4 °C and 12,000×*g*. A 5-μL aliquot of the recovered supernatant was saved and assayed for total protein by Pierce™ BCA Protein Assay Kit. Equal amounts of proteins (500–1000 μg) were incubated with gelatin-Sepharose 4B at 4 °C overnight with agitation. Then, after centrifugation for 2 min at 4 °C and 6 000×*g*, the supernatant was removed. The gelatin-Sepharose pellets were subjected to three cycles of washing with the working buffer, each followed by centrifugation under the same conditions. After the final wash, the gelatin-Sepharose pellets were incubated at 4 °C for 2 h with elution buffer consisting of the working buffer plus 10 % DMSO. The samples were mixed with 4 × sample buffer (0.2 M Tris-HCl, pH = 6.8, 8 % SDS, 40 % glycerol, and 0.008 % bromophenol blue), loaded on an 8 % polyacrylamide gel copolymerized with FITC-gelatin as a substrate and run for 3 h at 90 V. After electrophoresis, the SDS was removed from the gels by washing twice with zymogram renaturating buffer (2.5 % Triton X-100, 30 min each), and the gels were then incubated at 37 °C in a developing buffer containing 50 mM Tris-HCl, pH = 7.5, 1 % Triton X-100, 10 mM $CaCl_2$, 0.02 % NaN_3, and 1 μM $ZnCl_2$ for 48 h. Following incubation, the images of gels were acquired using a G:BOX Chemi

imaging system with transilluminator and an SW06 short-pass filter (495–600 nm; Syngene, Frederick, MD) and analyzed using ImageJ.

Statistical analysis was performed using GraphPad Prism8 software. The zymograms were quantitatively analyzed by the sum of replicates (each data point on a replicate is divided by the sum of the values of all data points in that replicate) [38]. Analysis of variance (ANOVA) followed by Tukey's multiple comparisons test was used for multiple comparisons.

CRediT authorship contribution statement

Vittorio Canale: Writing – review & editing, Writing – original draft, Methodology, Investigation, Conceptualization. **Klaudia Blicharz-Futera:** Methodology, Investigation. **Monika Bijata:** Methodology, Investigation, Data curation. **Natalie G. Cavalco:** Investigation. **Anna Partyka:** Methodology, Investigation, Data curation. **Matylda Stefaniak:** Investigation. **Michał Kamiński:** Investigation. **Grzegorz Satała:** Methodology, Investigation, Data curation. **Dawid Warszycki:** Methodology, Investigation, Data curation. **Janelle K. Lanham:** Investigation. **Joanna Gołębiowska:** Methodology, Investigation, Data curation. **Maciej Gawlik:** Investigation. **Magdalena Smolik:** Investigation. **Krystian Bijata:** Investigation. **Magdalena Jastrzębska-Więsek:** Investigation. **Rafał Kurczab:** Methodology. **Andrzej J. Bojarski:** Methodology. **Maria Walczak:** Methodology, Data curation. **John D. McCorvy:** Writing – review & editing, Methodology, Formal analysis, Data curation. **Jakub Włodarczyk:** Methodology. **Piotr Popik:** Writing – review & editing, Methodology, Formal analysis. **Paweł Zajdel:** Writing – review & editing, Writing – original draft, Supervision, Methodology, Funding acquisition, Conceptualization.

Declaration of competing interest

The authors declare that they have no known competing financial interests or personal relationships that could have appeared to influence the work reported in this paper.

Acknowledgments

The studies were funded by the National Science Centre, Poland, grant no 2019/33/B/NZ7/02822 (to PZ), by the National Institute of Mental Health (NIMH, USA) grant no NIMH R01MH133849 (to JDM) and by the National Institute of General Medical Sciences (NIGMS, USA), grant no NIGMS R35GM133421 (to JDM). Some of the experiments were carried out with equipment co-financed by the qLIFE Priority Research Area under the program "Excellence Initiative—Research University" at Jagiellonian University.

Appendix B. Supplementary data

Supplementary data to this article can be found online at https://doi.org/10.1016/j.ejmech.2025.118369.

Data availability

Data will be made available on request.

References

[1] N. Gottlieb, T.-Y. Li, A.H. Young, P.R. Stokes, The 5-HT$_7$ receptor system as a treatment target for mood and anxiety disorders: a systematic review, J. Psychopharmacol. 37 (2023) 1167–1181, https://doi.org/10.1177/02698811231211228.

[2] P.D. Harvey, The clinical utility of lurasidone in schizophrenia: patient considerations, Neuropsychiatr. Dis. Treat. 11 (2015) 1103–1109, https://doi.org/10.2147/NDT.S68417.

[3] R. Okubo, T. Hasegawa, K. Fukuyama, T. Shiroyama, M. Okada, Current limitations and candidate potential of 5-HT$_7$ receptor antagonism in psychiatric pharmacotherapy, Front. Psychiatry 12 (2021) 623684, https://doi.org/10.3389/fpsyt.2021.623684.

[4] K. Jahreis, A. Brüge, S. Borsdorf, F.E. Müller, W. Sun, S. Jia, D.M. Kang, N. Boesen, S. Shin, S. Lim, A. Koroleva, G. Satała, A.J. Bojarski, E. Rakuša, A. Fink, G. Doblhammer-Reiter, Y.K. Kim, A. Dityatev, E. Ponimaskin, J. Labus, Amisulpride as a potential disease-modifying drug in the treatment of tauopathies, Alzheimer's Dement. 19 (2023) 5482–5497, https://doi.org/10.1002/alz.13090.

[5] T.W. Lovenberg, B.M. Baron, L. de Lecea, J.D. Miller, R.A. Prosser, M.A. Rea, P. E. Foye, M. Racke, A.L. Slone, B.W. Siegel, A novel adenylyl cyclase-activating serotonin receptor (5-HT$_7$) implicated in the regulation of Mammalian circadian rhythms, Neuron 11 (1993) 449–458, https://doi.org/10.1016/0896-6273(93)90149-l.

[6] D. Guseva, A. Wirth, E. Ponimaskin, Cellular mechanisms of the 5-HT$_7$ receptor-mediated signaling, Front. Behav. Neurosci. 8 (2014) 306, https://doi.org/10.3389/fnbeh.2014.00306.

[7] M. Bijata, E. Bączyńska, F.E. Müller, K. Bijata, J. Masternak, A. Krzystyniak, B. Szewczyk, M. Siwiec, S. Antoniuk, M. Roszkowska, I. Figiel, M. Magnowska, K. H. Olszyński, A.D. Wardak, A. Hogendorf, B. Ruszczycki, N. Gorinski, J. Labus, T. Stępień, S. Tarka, A.J. Bojarski, K. Tokarski, R.K. Filipkowski, E. Ponimaskin, J. Wlodarczyk, Activation of the 5-HT$_7$ receptor and MMP-9 signaling module in the hippocampal CA1 region is necessary for the development of depressive-like behavior, Cell Rep. 38 (2022), https://doi.org/10.1016/j.celrep.2022.110532.

[8] E. Domenici, D.R. Willé, F. Tozzi, I. Prokopenko, S. Miller, A. McKeown, C. Brittain, D. Rujescu, I. Giegling, C.W. Turck, F. Holsboer, E.T. Bullmore, L. Middleton, E. Merlo-Pich, R.C. Alexander, P. Muglia, Plasma protein biomarkers for depression and schizophrenia by multi analyte profiling of case-control collections, PLoS One 5 (2010) e9166.

[9] P. Bonaventure, C. Dugovic, M. Kramer, P. De Boer, J. Singh, S. Wilson, K. Bertelsen, J. Di, J. Shelton, L. Aluisio, L. Dvorak, I. Fraser, B. Lord, D. Nepomuceno, A. Ahnaou, W. Drinkenburg, W. Chai, C. Dvorak, S. Sands, N. Carruthers, T.W. Lovenberg, Translational evaluation of JNJ-18038683, a 5-hydroxytryptamine type 7 receptor antagonist, on rapid eye movement sleep and in major depressive disorder, J. Pharmacol. Exp. Ther. 342 (2012) 429–440, https://doi.org/10.1124/jpet.112.193995.

[10] M. Arshadi, A.Z. Elmaadawi, S. Nasr, K. Jayathilake, S. Rassnick, L. Ford, W. C. Drevets, H.Y. Meltzer, Lack of efficacy of JNJ-18038683 on cognitive impairment in patients with stable bipolar disorder, J. Clin. Psychopharmacol. 44 (2024) 481–491, https://doi.org/10.1097/JCP.0000000000001889.

[11] P. Zajdel, R. Kurczab, K. Grychowska, G. Satała, M. Pawłowski, A.J. Bojarski, The multiobjective based design, synthesis and evaluation of the arylsulfonamide/amide derivatives of aryloxyethyl- and arylthioethyl- piperidines and pyrrolidines as a novel class of potent 5-HT$_7$ receptor antagonists, Eur. J. Med. Chem. 56 (2012) 348–360, https://doi.org/10.1016/j.ejmech.2012.07.043.

[12] P. Zajdel, V. Canale, A. Partyka, K. Marciniec, R. Kurczab, G. Satała, A. Siwek, M. Jastrzębska-Więsek, A. Wesołowska, T. Kos, P. Popik, A.J. Bojarski, Arylsulfonamide derivatives of (aryloxy)ethylpiperidines as selective 5-HT$_7$ receptor antagonists and their psychotropic properties, Med. Chem. Commun. 6 (2015) 1272–1277, https://doi.org/10.1039/C5MD00166H.

[13] A. Partyka, M. Jastrzębska-Więsek, L. Antkiewicz-Michaluk, J. Michaluk, A. Wąsik, V. Canale, P. Zajdel, M. Kołaczkowski, A. Wesołowska, Novel antagonists of 5-HT (6) and/or 5-HT(7) receptors affect the brain monoamines metabolism and enhance the anti-immobility activity of different antidepressants in rats, Behav. Brain Res. 359 (2019) 9–16, https://doi.org/10.1016/j.bbr.2018.10.004.

[14] V. Canale, R. Kurczab, A. Partyka, G. Satała, T. Lenda, M. Jastrzębska-Więsek, A. Wesołowska, A.J. Bojarski, P. Zajdel, Towards new 5-HT$_7$ antagonists among arylsulfonamide derivatives of (Aryloxy)ethyl-alkyl amines: multiobjective based design, synthesis, and antidepressant and anxiolytic properties, Eur. J. Med. Chem. 108 (2016) 334–346, https://doi.org/10.1016/j.ejmech.2015.11.040.

[15] V. Canale, A. Partyka, R. Kurczab, M. Krawczyk, T. Kos, G. Satała, B. Kubica, M. Jastrzębska-Więsek, A. Wesołowska, A.J. Bojarski, P. Popik, P. Zajdel, Novel 5-HT(7)R antagonists, arylsulfonamide derivatives of (aryloxy)propyl piperidines: add-on effect to the antidepressant activity of SSRI and DRI, and pro-cognitive profile, Bioorg. Med. Chem. 25 (2017) 2789–2799, https://doi.org/10.1016/j.bmc.2017.03.057.

[16] V. Canale, V. Frisi, X. Bantreil, F. Lamaty, P. Zajdel, Sustainable synthesis of a potent and selective 5-HT(7) receptor antagonist using a mechanochemical approach, J. Org. Chem. 85 (2020) 10958–10965, https://doi.org/10.1021/acs.joc.0c01044.

[17] V. Canale, M. Kamiński, W. Trybała, M. Abram, K. Marciniec, X. Bantreil, F. Lamaty, J.R. Parkitna, P. Zajdel, Multistep mechanochemical synthesis of PZ-1190, a multitarget antipsychotic agent, ACS Sustain. Chem. Eng. 11 (2023) 16156–16164, https://doi.org/10.1021/acssuschemeng.3c04023.

[18] P. Zajdel, K. Grychowska, S. Mogilski, R. Kurczab, G. Satała, R. Bugno, T. Kos, J. Gołębiowska, N. Malikowska-Racia, A. Nikiforuk, S. Chaumont-Dubel, X. Bantreil, M. Pawłowski, J. Martinez, G. Subra, F. Lamaty, P. Marin, A.J. Bojarski, P. Popik, Structure-based design and optimization of FPPQ, a dual-acting 5-HT(3) and 5-HT(6) receptor antagonist with antipsychotic and procognitive properties, J. Med. Chem. 64 (2021) 13279–13298, https://doi.org/10.1021/acs.jmedchem.1c00224.

[19] N.A. Meanwell, The influence of bioisosteres in drug design: tactical applications to address developability problems, tactics in contemporary drug design 9 (2015) 283–381, https://doi.org/10.1007/7355_2013_29.

[20] K.J. Bowers, E. Chow, H. Xu, R.O. Dror, M.P. Eastwood, B.A. Gregersen, J. L. Klepeis, I. Kolossvary, M.A. Moraes, F.D. Sacerdoti, J.K. Salmon, Y. Shan, D. E. Shaw, Scalable algorithms for molecular dynamics simulations on commodity

clusters, in: Proceedings of the ACM/IEEE Conference on Supercomputing (SC06), Tampa, Florida, 2006. November 11-17.
[21] Metasite, Molecular Discovery; Program, 2020 version 6.0.1.
[22] T. Ishibashi, T. Horisawa, K. Tokuda, T. Ishiyama, M. Ogasa, R. Tagashira, K. Matsumoto, H. Nishikawa, Y. Ueda, S. Toma, H. Oki, N. Tanno, I. Saji, A. Ito, Y. Ohno, M. Nakamura, Pharmacological profile of lurasidone, a novel antipsychotic agent with potent 5-hydroxytryptamine 7 (5-HT_7) and 5-HT_{1A} receptor activity, J. Pharmacol. Exp. Ther. 334 (2010) 171–181, https://doi.org/10.1124/jpet.110.167346.
[23] T. Karcz, K. Szczepańska, S. Mogilski, A. Moroz, A. Olejarz-Maciej, L.J. Humphrys, S. Pockes, A. Siwek, K. Dubiel, M. Staszewski, T. Calmels, K. Waczyński, K. Kieć-Kononowicz, Guanidine derivative ADS1017, a potent histamine H_3 receptor antagonist with promising analgesic activity and satisfactory safety profile, ACS Chem. Neurosci. 15 (2024) 4441–4457, https://doi.org/10.1021/acschemneuro.4c00480.
[24] G.M. Sastry, M. Adzhigirey, T. Day, R. Annabhimoju, W. Sherman, Protein and ligand preparation: parameters, protocols, and influence on virtual screening enrichments, J. Comput. Aided Mol. Des. 27 (2013) 221–234, https://doi.org/10.1007/s10822-013-9644-8.
[25] R.C. Johnston, K. Yao, Z. Kaplan, M. Chelliah, K. Leswing, S. Seekins, S. Watts, D. Calkins, J. Chief Elk, S. V Jerome, M.P. Repasky, J.C. Shelley, Epik: pk(a) and protonation state prediction through machine learning, J. Chem. Theory Comput. 19 (2023) 2380–2388, https://doi.org/10.1021/acs.jctc.3c00044.
[26] Y. Yang, K. Yao, M.P. Repasky, K. Leswing, R. Abel, B.K. Shoichet, S.V. Jerome, Efficient exploration of chemical space with docking and deep learning, J. Chem. Theory Comput. 17 (2021) 7106–7119, https://doi.org/10.1021/acs.jctc.1c00810.
[27] R.A. Friesner, R.B. Murphy, M.P. Repasky, L.L. Frye, J.R. Greenwood, T.A. Halgren, P.C. Sanschagrin, D.T. Mainz, Extra precision glide: docking and scoring incorporating a model of hydrophobic enclosure for protein-ligand complexes, J. Med. Chem. 49 (2006) 6177–6196, https://doi.org/10.1021/jm051256o.
[28] R. Kurczab, V. Canale, G. Satała, P. Zajdel, A.J. Bojarski, Amino acid hot spots of halogen bonding: a combined theoretical and experimental case study of the 5-HT (7) receptor, J. Med. Chem. 61 (2018) 8717–8733, https://doi.org/10.1021/acs.jmedchem.8b00828.
[29] M. Drop, V. Canale, S. Chaumont-Dubel, R. Kurczab, G. Satała, X. Bantreil, M. Walczak, P. Koczurkiewicz-Adamczyk, G. Latacz, A. Gwizdak, M. Krawczyk, J. Gołębiowska, K. Grychowska, A.J. Bojarski, A. Nikiforuk, G. Subra, J. Martinez, M. Pawłowski, P. Popik, P. Marin, F. Lamaty, P. Zajdel, 2-Phenyl-1H-pyrrole-3-carboxamide as a new scaffold for developing 5-HT(6) receptor inverse agonists with cognition-enhancing activity, ACS Chem. Neurosci. 12 (2021) 1228–1240, https://doi.org/10.1021/acschemneuro.1c00061.
[30] Y. Cheng, W.H. Prusoff, Relationship between the inhibition constant (K1) and the concentration of inhibitor which causes 50 per cent inhibition (I50) of an enzymatic reaction, Biochem. Pharmacol. 22 (1973) 3099–3108, https://doi.org/10.1016/0006-2952(73)90196-2.
[31] J.K. Singh, A. Solanki, V.S. Shirsath, Comparative in-vitro intrinsic clearance of imipramine in multiple species liver microsomes: human, rat, mouse and dog, J. Drug Metab. Toxicol. 3 (2012) 1–6.
[32] V. Canale, W. Trybała, S. Chaumont-Dubel, P. Koczurkiewicz-Adamczyk, G. Satała, O. Bento, K. Blicharz-Futera, X. Bantreil, E. Pękala, A.J. Bojarski, F. Lamaty, P. Marin, P. Zajdel, 1-(Arylsulfonyl-isoindol-2-yl)piperazines as 5-HT(6)R antagonists: mechanochemical synthesis, in vitro pharmacological properties and glioprotective activity, Biomolecules 13 (2022), https://doi.org/10.3390/biom13010012.
[33] V. Lewis, E.M. Bonniwell, J.K. Lanham, A. Ghaffari, H. Sheshbaradaran, A.B. Cao, M.M. Calkins, M.A. Bautista-Carro, E. Arsenault, A. Telfer, F.-F. Taghavi-Abkuh, N. J. Malcolm, F. El Sayegh, A. Abizaid, Y. Schmid, K. Morton, A.L. Halberstadt, A. Aguilar-Valles, J.D. McCorvy, A non-hallucinogenic LSD analog with therapeutic potential for mood disorders, Cell Rep. 42 (2023) 112203, https://doi.org/10.1016/j.celrep.2023.112203.
[34] H.C. Cheng, The power issue: determination of K_B or K_i from IC_{50}. A closer look at the cheng-prusoff equation, the schild plot and related power equations, J. Pharmacol. Toxicol. Methods 46 (2001) 61–71, https://doi.org/10.1016/s1056-8719(02)00166-1.
[35] R.D. Porsolt, A. Bertin, M. Jalfre, Behavioral despair in mice: a primary screening test for antidepressants, Arch. Int. Pharmacodyn. Ther. 229 (1977) 327–336.
[36] P. Popik, M. Hołuj, A. Nikiforuk, T. Kos, R. Trullas, P. Skolnick, 1-aminocyclopropanecarboxylic acid (ACPC) produces procognitive but not antipsychotic-like effects in rats, Psychopharmacology (Berl) 232 (2015) 1025–1038, https://doi.org/10.1007/s00213-014-3738-4.
[37] A. Ennaceur, J. Delacour, A new one-trial test for neurobiological studies of memory in rats. 1: behavioral data, Behav. Brain Res. 31 (1988) 47–59, https://doi.org/10.1016/0166-4328(88)90157-x.
[38] A. Degasperi, M.R. Birtwistle, N. Volinsky, J. Rauch, W. Kolch, B.N. Kholodenko, Evaluating strategies to normalise biological replicates of Western blot data, PLoS One 9 (2014) e87293, https://doi.org/10.1371/journal.pone.0087293.